3. SITE 487[1]

Shipboard Scientific Party[2]

HOLE 487

Date occupied: 24 March 1979

Date departed: 27 March 1979

Time on hole: 63.2 hours

Position: 15°51.21′N; 99°10.52′W

Water depth (sea level; corrected m, echo-sounding): 4764

Water depth (rig floor; corrected m, echo-sounding): 4774

Bottom felt (m, drill pipe): 4777

Penetration (m): 181.7

Number of cores: 21

Total length of cored section (m): 181.7

Total core recovered (m): 119.9

Core recovery (%): 66

Oldest sediment cored:
Depth sub-bottom (m): 170
Nature: Brown clay
Age: Late Miocene

Basement:
Depth sub-bottom (m): 171
Nature: Basalt

Principal results: Site 487 drilling penetrated 171 meters of sediments before bottoming in basalt of late Miocene age (Table 1). The near-absence of carbonate microfossil remains suggests deposition of the entire sequence below the carbonate compensation depth (CCD) despite deposition of the lowermost part of the section at or near the crest of the East Pacific Rise. Paleomagnetic polarity measurements were consistent with paleontological data and significantly improved the precision with which the section was dated.

The sedimentary section consisted of Quaternary hemipelagic gray mud 105 meters thick overlying upper Miocene–Pliocene pelagic brown clay.

Sedimentation rates in the lower unit were a relatively high 29 m/m.y. near the ridge crest but diminished to 7 m/m.y., which may be due in part to carbonate solution with increasing water depths as the crust moved away from the ridge crest. The oldest hemipelagic sediments may have been deposited 100 km from the trench axis and at an elevation approximately 1000 meters above the present trench floor. The sedimentation rate increased rapidly in the upper units, attaining its current level of 126 m/m.y. about 30 km from the trench.

Figure 1 summarizes findings at Site 487.

Table 1. Coring summary, Hole 487.

Core	Cored Interval below Bottom (m)	Cored (m)	Recovered (m)	Recovered (%)	Remarks
1	0.0–1.0	1.0	0.26	26	Gray mud
2	1.0–10.5	9.5	9.03	95	Gray mud
3	10.5–20.0	9.5	8.03	85	Gray mud
4	20.0–29.5	9.5	tr	—	Gray mud
5	29.5–39.0	9.5	4.52	48	Gray mud
6	39.0–48.5	9.5	5.17	54	Gray mud
7	48.5–58.0	9.5	6.04	64	Gray mud
8	58.0–67.5	9.5	8.63	91	Gray mud
9	67.5–77.0	9.5	9.55	101	Gray mud
10	77.0–86.5	9.5	9.68	102	Gray mud
11	86.5–96.0	9.5	6.30	66	Gray mud
12	96.0–105.5	9.5	6.71	71	Gray mud
13	105.5–115.0	9.5	6.54	69	Gray mud
14	115.0–124.5	9.5	5.38	57	Brown clay
15	124.5–134.0	9.5	9.59	101	Brown clay
16	134.0–143.5	9.5	6.27	66	Brown clay
17	143.5–153.0	9.5	2.36	25	Brown clay
18	153.0–162.5	9.5	9.20	97	Brown clay
19	162.5–172.0	9.5	4.82	51	Change in drilling resistance
20	172.0–181.5	9.5	1.70	18	at 171 meters interpreted as
21	181.5–190.5	9.5	0.20	2	initial contact with basement.
			119.38	63	Basalt recovered in Cores 20 and 21 only.

BACKGROUND AND OBJECTIVES

The hypothesis on accretion predicts that sediment deposited on oceanic crust will be scraped off and, together with trench and lower slope sediments, incorporated into the inner trench walls. In addition, some sediment may be carried into the subduction zone beneath the accretionary zone and either underplate that zone or be consumed in the subduction process.

Understanding the partitioning of sediment flux during subduction depends on recognition of the provenance of accretionary zone sediments. It is thus important to obtain samples of unaltered sediments from the different depositional environments in order to recognize their altered equivalents. Site 487 addresses this problem as it samples the unaccreted pelagic and hemipelagic sediment from the oceanic crust seaward of the trench (Fig. 2).

The specific objective at Site 487 was the coring of pelagic and hemipelagic sediment section and underlying oceanic basement. These cores provide a reference section for use in determining the amount of the oceanic crustal pelagic–hemipelagic sediment input into the ac-

[1] *Initial Reports of the Deep Sea Drilling Project*, Volume 66.

[2] Joel S. Watkins (Co-Chief Scientist), Gulf Research and Development Company, Houston, Texas (present address: Geology and Interpretation Department, Exploration and Production Division, Gulf Science and Technology Company, Pittsburgh, Pennsylvania); J. Casey Moore (Co-Chief Scientist), Earth Sciences Board, University of California, Santa Cruz, California; Steven B. Bachman, Department of Geology, University of California, Davis, California (present address: Department of Geological Sciences, Cornell University, Ithaca, New York); Floyd W. Beghtel, Phillips Petroleum Company, Bartlesville, Oklahoma; Arif Butt, Institut und Museum für Geologie und Paläontologie, Universität Tübingen, Tübingen, Federal Republic of Germany; Borys M. Didyk, Research and Development Laboratory, Empresa Nacional del Petróleo (ENAP), Concon, Chile; Glen Foss, Deep Sea Drilling Project, Scripps Institution of Oceanography, La Jolla, California; Jeremy K. Leggett, Department of Geology, Imperial College of Science and Technology, London, United Kingdom; Neil Lundberg, Earth Sciences Board, University of California, Santa Cruz, California; Kenneth J. McMillen, Geophysics Laboratory, Marine Science Institute, University of Texas, Galveston, Texas (present address: Geology and Interpretation Department, Exploration and Production Division, Gulf Science and Technology Company, Pittsburg, Pennsylvania); Nobuaki Niitsuma, Institute of Geosciences, Shizuoka University, Oya, Shizuoka, Japan; Les E. Shephard, Department of Oceanography, College of Geosciences, Texas A&M University, College Station, Texas (present address: Sandia National Laboratories, Division 4536, Albuquerque, New Mexico); Jean-François Stephan, Département de Géotectonique, Université Pierre et Marie Curie, Paris, France; Thomas H. Shipley, Scripps Institution of Oceanography, University of California at San Diego, La Jolla, California; and Herbert Stradner, Geologische Bundesanstalt, Vienna, Austria.

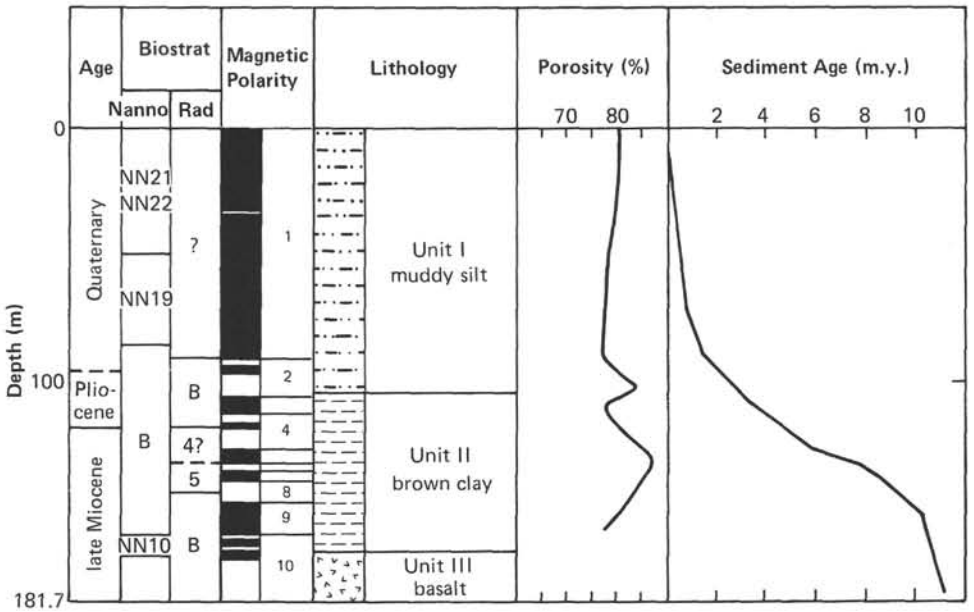

Figure 1. Summary age, nannofossil and radiolarian zones (4 = *Ommatartus penultimus*, 5 = *O. antepenultimus*, B = barren), magnetic polarity zones (black = normal polarity), lithology, porosity, and age–depth relationships of sediments recovered at Site 487. Slope of age–depth curve equals sediment accumulation rate uncorrected for compaction. (Radiolarian and nannofossil boundaries are based on Berggren and Van Couvering [1974] and paleomagnetic ages on Ryan et al. [1974].)

cretionary zone section relative to input from trench wedge turbidites, the downslope apron, and slope basins.

In a broader context, data from Site 487 help resolve the problem of consumption of sediments during the subduction process. Volume, age, and type of sediment overlying oceanic crust coupled with similar information from the trench and slope permit estimation of the sediment budget during the accretionary process, an essential consideration in estimating relative amounts of sediment being accreted and consumed.

In addition to contributing to determination of the sediment budget, Site 487 cores serve as a baseline for observations of dewatering, compaction, tectonic alteration, and diagenesis of accretionary zone sediments. Alteration of accretionary zone sediments is thought to be broadly time-progressive, and, if the imbricate thrust model of accretion is correct, sediment alteration and age will increase progressively up the slope. Without baseline data for unaltered sediments from trench and oceanic crust sites, measurement of sediment alteration becomes relative rather than absolute. Baseline data are particularly important near the base of the slope where slight increases in seismic velocities relative to velocities in unaltered sediments may indicate subtle alteration.

On a regional basis, Site 487 lithologies, ages, and faunal assemblages provide a record of the history and evolution of the northern Cocos Plate. Site 487 cores give the age of oceanic crust, environments of deposition, and sediment accumulation rates, all of which are important to the reconstruction of the geologic history of the region.

Finally, Site 487 cores contribute to a subsidiary objective of Leg 66 drilling—the investigation of gas hydrates in the accretionary zone. The source of the methane, from which the hydrates are thought to derive, remains unclear. They could derive from alteration of organic matter entrapped by trench turbidites, organic matter enclosed by oceanic mantling sediments, or from primary methane production from within oceanic crust. Determination of content and isotopic composition of organic matter within trench and crust sediments will constrain methane source models.

OPERATIONS

Moving the *Challenger* to the beacon drop point 4 miles southwest of Site 486 over a small basin of relatively thin sediments required 2½ hours. The beacon was dropped at 1338 hours on March 24, and the pipe trip began an hour later after seismic gear had been retrieved and positioning established. A 2¼-hour pressure core barrel test was conducted during the pipe trip.

A mudline punch core established water depth at 4777 meters, whereas the PDR reading was 4774 meters. The coarse, loose sands we encountered at Site 486 were absent at the new location, and continuous coring proceeded in soft mud. The sediment changed little in character with depth; the much older material at the basement contact was only semiconsolidated. We hit weathered rubbly basalt at approximately 171 meters BSF.

After about 10 meters of basalt had been cored, a breakdown and loss of power to the Bowen hydraulic system halted operations. Although we needed two additional cores to provide sufficient basalt penetration for meaningful well logs, we terminated operations without logging when, after 5 hours, the electrical problem had still not been solved. We recovered the drill string, and the vessel got underway at 0450 hours, March 27, 1979.

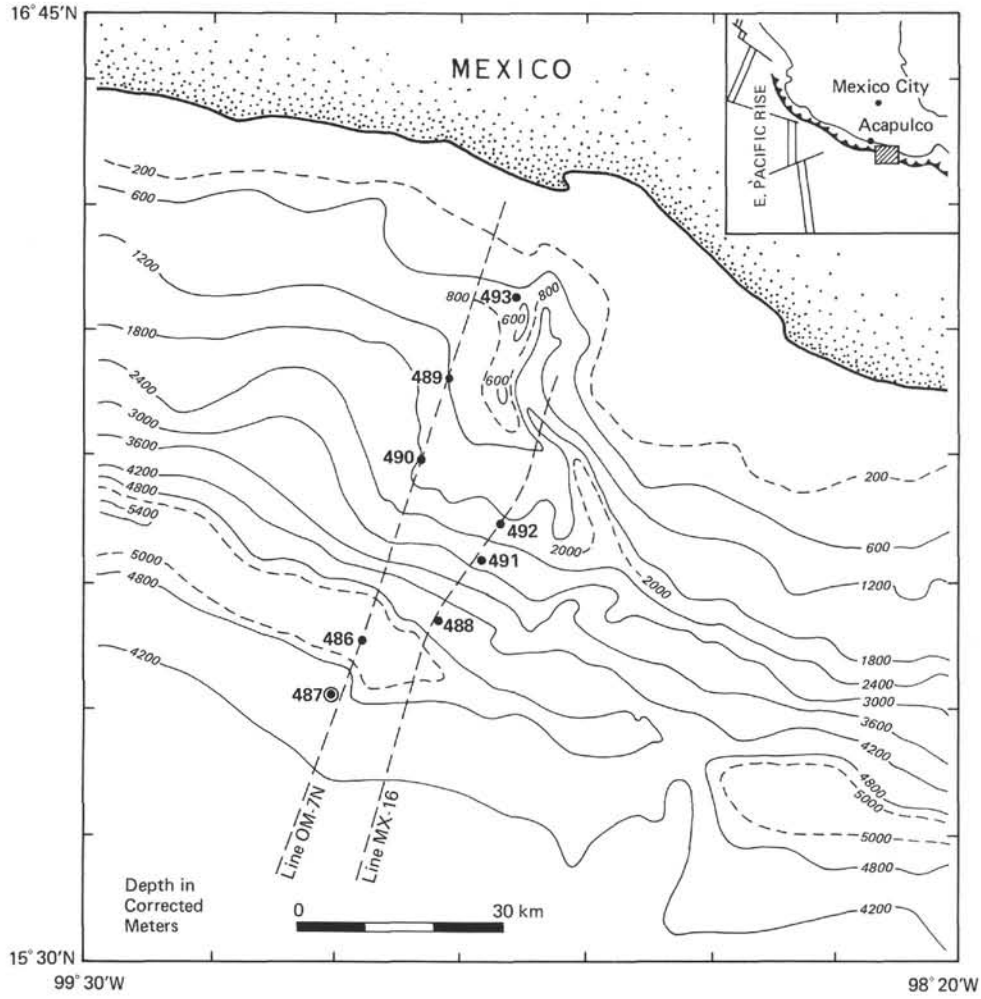

Figure 2. Location of Site 487 and site survey reflection lines.

LITHOLOGIC SUMMARY

Hole 487 penetrated about 171 meters of unconsolidated pelagic and hemipelagic sediments and about 20 meters of basaltic basement. Two units (from top to base), 1 and 2, can be distinguished in the sedimentary sequence (Fig. 3; Chart 1, back pocket):

Unit 1, Quaternary (Cores 1–12, 0–105.5 m sub-bottom), is composed mainly of gray hemipelagic mud (locally muddy silt). Smear slides and grain-size analysis show the silt fraction usually between 20% and 60%. Both silt and clay material are dominantly quartz, feldspars, and mica. Calcareous and siliceous microfossils are present.

Unit 2, upper Miocene and Pliocene (Cores 13–19, 105.5–171.0 m sub-bottom), is composed mainly of brown pelagic clay (65 m thick), except in Core 13, where gray clay represents the transition between Unit 1 and Unit 2. In smear slides the dominantly brown clay accounts for more than 95% (silt = 5%) of the material. Zeolites (phillipsite?) are present and may form small nodules. Microfossils are exclusively siliceous in the uppermost Miocene–Pliocene section, and calcareous microfossils (pelagic foraminifers and coccoliths) reappear in the lower part of the upper Miocene section immediately above the basement.

The contact between the two units is evident from both the change in color (gray above, brown below) and the silt/clay ratio observed in smear slides.[3]

Both sedimentary units contain ash layers; at least two have been identified in the Miocene–Pliocene unit and five in the Quaternary unit. Volcanic glass is present in minor amounts throughout most of the section.

The following are our three main conclusions:

1) Middle Miocene age, suggested for the oceanic crust by magnetic anomalies (Lynn and Lewis, 1976, Fig. 2), is consistent with recovery of upper Miocene sediments above the presumed basement.

2) Discrete ash layers and minor amounts of volcanic glass throughout the section (Fig. 4) probably represent the effects of active volcanism in western Mexican borderlands during the Oligo–Miocene (andesites and ignimbrites of the Sierra Madre Occidental and Sierra Madre del Sur) and Plio–Quaternary (andesites and basalts of the Trans-Mexican Neovolcanic Belt and

[3] In Unit 2, data from grain-size analysis have not been used; see explanation in the Introductory Notes.

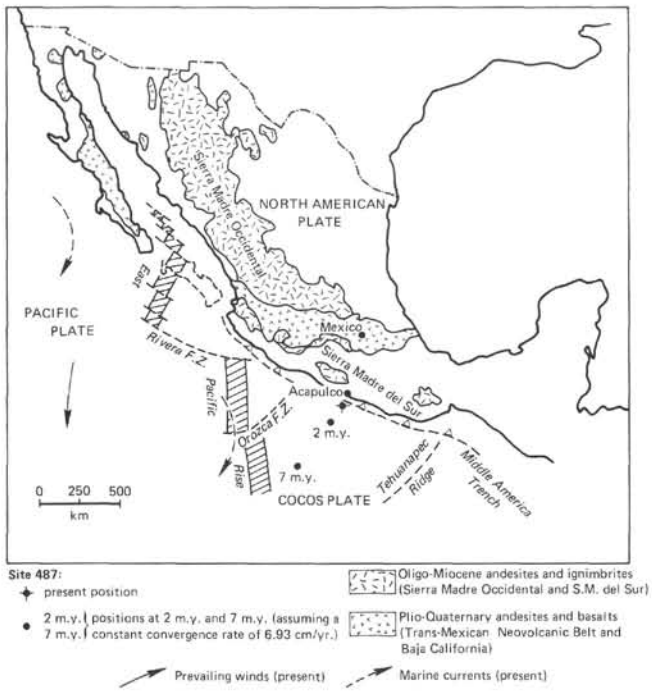

Figure 4. Possible sources for the ash layers at Site 487 (data on relative motion between North American Plate and Cocos Plate are from Minster and Jordan, 1978).

eastern border of Baja California; Tardy, 1977). Northerly prevailing winds and north-to-south and northwest-to-southeast ocean currents may account for the ash dispersal, even though Site 487 may have been about 400 km southwest of its present position in the late Miocene (see the following). A west-southwest source (from former volcanic islands) cannot be totally excluded, particularly for the upper Miocene section of Site 487 when it was near the East Pacific Rise.

3) The evolution of the sedimentary sequence from base to top reflects the horizontal passage from an oceanic pelagic environment (ridge axis, ridge flank, ocean floor) to a hemipelagic environment adjacent to the trench.

If we assume (Minster and Jordan, 1978) a constant convergence rate of 6.93 cm/y. at 038° for the Cocos Plate, Site 487 can be relocated 7 and 2 Ma (Fig. 4). Prior to 7 Ma, the position of Site 487 is more difficult to determine because of uncertainties in direction and rate of spreading along the East Pacific Rise. The pelagic (Unit 2)–hemipelagic (Unit 1) facies change occurred 2 Ma. From 7 to 2 Ma, Site 487 moved from 485 to 140 km southwest of its present position. Brown pelagic clay accumulated during this time interval, although deposition began earlier—in middle (?) Miocene time. After 2 m.y., very fine terrigenous particles from the Mexican margin appear in the sediments. The percentage of silt increases to more than 5%, changing the pelagic clay to hemipelagic mud. At 0.3 Ma Site 487 was located about 20 km southwest of its present position. Sediment from that period of deposition shows more than 20% silt, owing to proximity to the trench with its continual turbidite flow. Later, when it reached the present trench, Site 487 was covered by sandy sediments.

BIOSTRATIGRAPHY

Site 487, located seaward of the Middle America Trench, was drilled to basement through a complete upper Miocene to Quaternary hemipelagic and pelagic sequence. Because of dissolution below the CCD, the pelagic sequence contains no calcareous microfossils. Some (possibly reworked) planktonic foraminifers and calcareous nannoplankton at the base of Site 487 indicate late Miocene deposition. Calcareous microfossils occur in the hemipelagic Quaternary section from Cores 1 to 9, possibly preserved because of more rapid burial by terrigenous sediments. Radiolarians occur sporadically throughout the section at Site 487 and are the only microfossil group used to zone much of the pelagic and hemipelagic interval from Cores 9 through 18.

Calcareous Nannoplankton

Quaternary calcareous nannoplankton occur in meager quantities from Cores 1 to 10. The dominant genus in all the assemblages is *Gephyrocapsa* with *G. oceanica* and *G. omega.*

Cores 1 to 7 are assigned to the *G. oceanica* nannoplankton zone (NN20) in the late part of the Quaternary. These nannoplankton assemblages were deposited after the extinction of *Emiliania annula* (= *Pseudoemiliania lacunosa*). Cores 8 to 10 are assigned to the *G. caribbeanica* subzone of the *G. doronicoides* Zone (Bukry, 1973) or the *Pseudoemiliania lacunosa* Zone (NN19) of the standard nannoplankton zonation (Martini, 1971). The latter zonal nannofossil is very rare among the dominant *Gephyrocapsa* coccoliths. In addition to *E. annula* and the *Gephyrocapsa* species *G. oceanica*, there are *G. caribbeanica* and *G. doronicoides.* There are also rare *Helicosphaera carteri* and a few reworked Mesozoic coccoliths (*Watznaueria barnesae*). The *G. doronicoides* nannoplankton zone of Bukry extends from the higher part of the early Quaternary to the middle Quaternary. Nannoplankton from the earliest Quaternary and Pliocene are not present.

The soupy and sandy parts of Cores 19 and 20 contain late Miocene nannoplankton. Discoasters and coccoliths are partly etched, partly overgrown. The assemblages contain *Discoaster exilis, D. variabilis, D. calcaris, D. bollii, D. stellulus, D. pentaradiatus, Sphenolithus abies, Triquetrorhabdulus rugosus,* and common *Coccolithus miopelagicus, Cyclicargolithus floridanus,* and *Coronocyclus* sp. (= *?Craspedolithus ragulus.*) The age assignment for this nannoplankton assemblage, which may be reworked, is late Miocene nannoplankton zone NN9/NN10. Those parts of the cores that are clayey and layered do not contain a calcareous fraction and are barren also in respect to siliceous phytoplankton.

Foraminifers

At Site 487, Cores 1 through 13 contain a dark greenish gray silty mud facies and Cores 14 through 18 a brown clay overlying basaltic basement. The sediments

of Site 487 are very poor in foraminifers; the brown clay is barren of calcareous microfossils, although some radiolarians, fish teeth, and sponge spicules occur. Interestingly, in Cores 19 and 20 a few well-preserved planktonic foraminifers were recovered.

The paucity of planktonic foraminifers and lack of index species do not permit us to apply the standard foraminiferal zonation. Nevertheless, the following species indicate a Quaternary age for Cores 1 through 8: *Globorotalia tumida, G. menardii, Globigerinoides triloba, G. ruber, Neogloboquadrina humerosa, Globigerina falconensis*, and *Orbulina universa*. These foraminifers represent a tropical assemblage identical to the assemblage in the trench fill sediments at Site 486.

The planktonic foraminifers recovered in the sand fraction of Samples 487-19-3, 100–110 cm and 487-20-1, 138–140 cm indicate late Miocene age for Cores 19 and 20. Important species include *Globorotalia acostaensis, G. continuosa, Globigerina venezuelana, G. nepenthes, Globoquadrina altispira*, and *Orbulina* sp.

Depositional Environment

Benthic foraminifers indicate reworked slope (bathyal) faunal associations. They were probably displaced by bottom currents or turbidity currents and redeposited at the present abyssal depth. Some of the typical forms are *Melonis pompilioides, Gyroidina* aff. *soldanii, Pullenia bulloides, Oridorsalis umbonatus, Cibicidoides*, and *Pseudonodosaria*.

Absence of planktonic foraminifers in the lower part of the section (brown clay) at Site 487 indicates that they were dissolved below the CCD during the Miocene–Pliocene. Occurrence of some well-preserved planktonic foraminifers in soupy portions of Cores 19 and 20 suggests that they were redeposited or that deposition occurred above the CCD at a ridge near the East Pacific Rise. During the plate movement the site probably subsided below the CCD. During the Quaternary, however, sporadic occurrences of planktonic foraminifers along with some calcareous benthic foraminifers (see the foregoing) suggest that these calcareous fossils escaped dissolution by rapid burial below the CCD by turbidity currents. The high sedimentation rate increase during the Quaternary is consistent with this hypothesis.

Radiolarians

Radiolarians at Site 487 are common to abundant in the upper part of the hole down to Core 7, but from Cores 7 through 12 they are rare to few. Below Core 12 radiolarians are absent to just above the base of Core 14, then rare through Core 17. From Core 17 to Core 19 only a few are present. Preservation of radiolarians is good in the upper part of Site 487 to Core 13 and in Cores 16 and 17 but poor elsewhere. These changes in abundance and preservation correlate with changes in sedimentation and sedimentation rate. Abundant, well-preserved radiolarians occur in greenish gray silty mud in Cores 1 through 5; fewer but still well-preserved radiolarians occur in Cores 6 through 12, where the silt content of the sediment decreases. Red and dark brown clays contain very few well-preserved radiolarians. Some red clay and all the gray clay below Core 12 are barren of radiolarians or contain only a few broken pieces of robust orosphaerid mesh. Increased abundance and better radiolarian preservation in the gray mud in Cores 1 through 12 might be due to rapid burial with terrigenous sediment, which hinders seafloor silica dissolution. The increased radiolarian abundance in Cores 1 through 5 might be due to (1) changes in productivity at the core site because of an increase in productivity in the east Pacific in the late Quaternary or because of movement of the core site on the Cocos Plate to a high productivity upwelling zone close to Mexico or to (2) an increase in the amount of resedimented Quaternary radiolarians originating on the inner slope and carried out by turbidity currents. The coincidence of the increase in radiolarian abundance with an increase in the silt content of the sediment supports the resedimentation hypothesis, but the abruptness of the abundance change and the loss of open ocean radiolarians such as *Collosphaera tuberosa* suggest a change in productivity due to upwelling.

The radiolarian biostratigraphy is summarized in Figure 1. The upper portion of Site 487 contains a Quaternary fauna, but because *C. tuberosa* and *Buccinosphaera invaginata* are absent, Nigrini's (1971) zonation cannot be applied to Cores 1 through 7. *C. tuberosa* is present only in Sample 487-6,CC. Sample 487-9,CC marks the last occurrence of *Axoprunum angelinum* (0.4 Ma, Hays, 1970). Core 13 and the upper part of Core 14 are barren of radiolarians. Because of the presence of *Ommatartus avitus* and the absence of *O. penultimus*, Sample 487-14,CC may be in the *Spongaster pentas* Zone (Pliocene). The Quaternary/Pliocene boundary is between Samples 487-12,CC and 14,CC. Because of the presence of *Stichocorys delmontensis*, possible early forms of *O. avitus*, and the absence of *O. hughesi* (Riedel and Sanfilippo, 1971; Dinkelman, 1973), we assign Sample 487-15-3, 59–61 cm to the *O. penultimus* Zone (upper Miocene). We infer from the abundance of *O. hughesi* (Dinkelman, 1973) that Cores 16 and 17 are all probably in the *O. antepenultimus* Zone (upper Miocene). This places the boundary between the *O. penultimus* and *O. antepenultimus* zones (8.7 Ma) at 130 meters. Below Core 17 a very few radiolarians indicate continuation of the *O. antepenultimus* Zone to the base of Core 19, immediately above oceanic basement.

SEDIMENT ACCUMULATION RATES

A sedimentation rate curve for Site 487, based on biostratigraphic data and paleomagnetic reversals, is shown in Figure 5. The average sediment accumulation rate of the gray mud in Cores 1 to 10 is 126 m/m.y.; the rate in the interval of gray mud and reddish brown clay decreases to 7 m/m.y.; and below Core 18 the rate increases in the dark brown clay to 29 m/m.y.

PALEOMAGNETISM

Quaternary and Neogene sediments and rocks at Site 487 recorded a geomagnetic field reversal sequence that

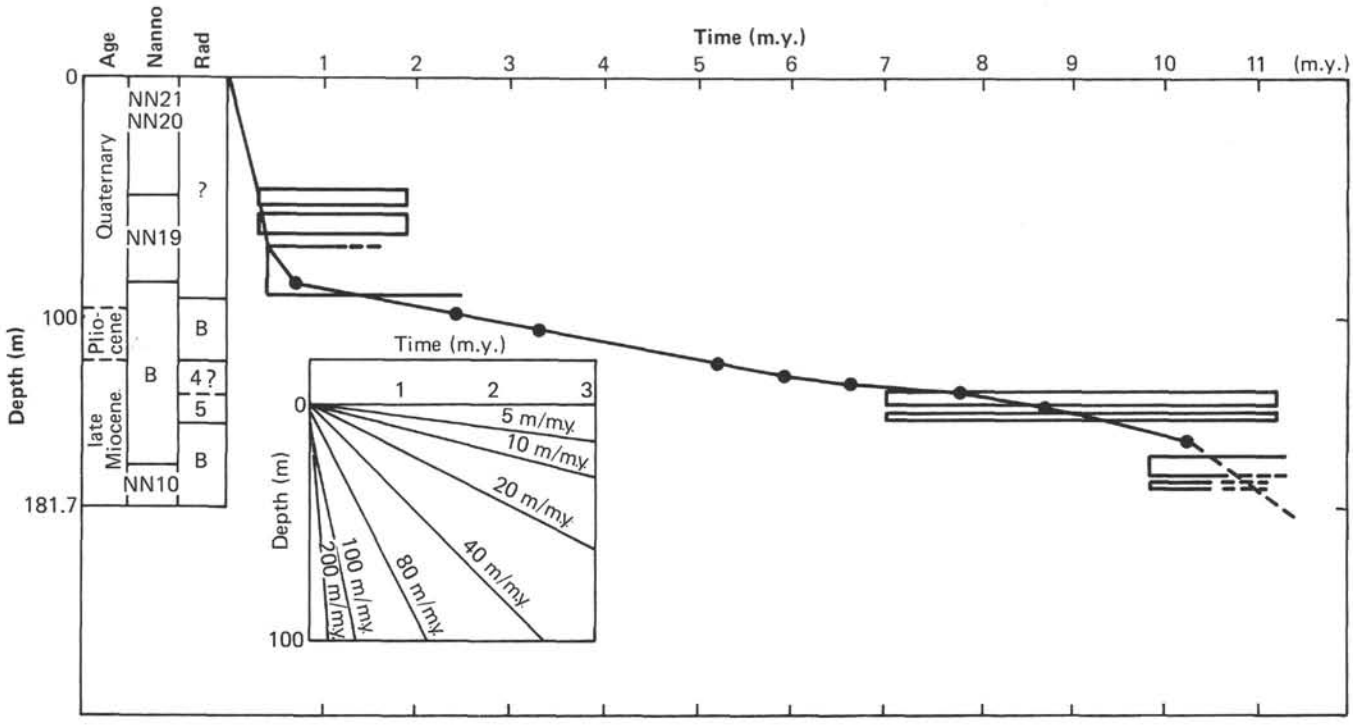

Figure 5. Age vs. depth of Site 487 samples. Boxes indicate faunal ranges. B indicates barren.

can be correlated with Brunhes normal polarity epoch to Epoch 10 (Fig. 1).

Fifty-one samples from the less disturbed parts of each section below 15 meters sub-bottom were collected for investigation. Oriented samples were placed in a plastic vial (2.4 cm in inner diameter and 2.2 cm in length). Because the stepwise AF demagnetization results of selected samples indicated that an unstable component of remanent magnetization could be eliminated by 5 to 15 mT AF demagnetization, all sediment samples were routinely cleaned with 15 mT AF demagnetization (Niitsuma, this volume).

Intensity of remanent magnetization of sediments ranged from 0.4 to 17.0 $\times 10^{-6}$ emu/cc after 15 mT AF demagnetization. Inclinations of the upper half sequence are positive except for one horizon at 31.65 meters. Below 89 meters we find an alternating sequence of reversed and normal polarities (Fig. 1). The upper 88-meter sequence of normal polarity can be correlated to the Brunhes normal polarity epoch. This correlation is supported by nannoplankton and radiolarian fossil data. Below the section of Brunhes Epoch, the normal and reversed polarity sequences supplemented by radiolarian, nannoplankton, and foraminiferal data are correlated with Matuyama reversed polarity epoch to Epoch 10.

Three samples were taken from the largest pieces of basalt recovered in Core 20 (Pieces 2, 13, and 17) with minicore drill, 2.54 cm in diameter, and then sawed 2.2 cm of length. Piece 2 is the only one large enough not to have rotated significantly in the barrel. The intensity of natural remanent magnetization (NRM) is 3.79 $\pm$ 0.81 $\times 10^{-3}$ emu/cc, and the mean demagnetizing field (MDF: the value of peak alternating field required to reduce the intensity of remanence to half of NRM) was 35 to 65 mT. The direction of the remanence is stable and the change in both inclination and declination is less than 5°. The magnetic minerals in the basalt samples are titanomaghemite with titanomagnetite. The inclination of the largest piece of basalt is $-28.8 \pm 0.2°$. These values are in fairly good agreement with the inclination of reversed axial dipole in the latitude of this site ($I = -29.50°$). Since the sand layer below the basalt contains the same microfossils as the brown pelagic clay above it, the basalt can be correlated with Epoch 10.

ORGANIC GEOCHEMISTRY

We carried out the shipboard organic geochemistry program by monitoring gases released in core liners, degasification of selected sediment samples, and visual inspection for fluorescence in split core.

Gases

We observed no appreciable amounts of gas within the sedimentary sequence. No gas release was observed by expansion of the core in the core liner, nor was pressure buildup in the core caps detected. These observations indicate that pore fluids were below gas saturation at ambient conditions upon core retrieval. Degasification of sediments by high-speed blending and analysis of released gases showed no evidence of light hydrocarbons (C_1 to C_5) or H_2S. The actual amount of C_1 present was below the detection limit 10 μl C/ml of sediment, with a gas-generating ratio $< 10^{-4}$. The only gas detected was CO_2, which varied from 3.9 to 38.1 μl CO_2/ml of sediment within the section cored. The amount of CO_2 released remained fairly constant with depth, showing a maximum near 119 meters, which can

be correlated with a change in lithology from a gray hemipelagic mud to a brown pelagic clay (see Lithologic Summary).

Fluorescence

Split cores showed no evidence of crude oil or bitumen impregnation. Fluorescent (white) droplets and superficial fluorescent stains observed on the surface of the Cores 1 and 8 and their core liners were probably due to contaminants from drilling fluids.

Organic Carbon, Nitrogen, and Carbonates

We observed neither evidence of organic gases nor spontaneous release of gases at this site. The only gas detected by forced degasification was CO_2.

C/N varies from 4.7 to 12.4. This is in the range for organic matter associated with recent sediments (Fairbridge, 1972) and suggests that the organic matter present in these sediments has a low degree of geothermal maturation. The decrease in C/N (Fig. 6) at about 100 meters corresponds to a change from hemipelagic gray mud (Unit 1) to brown pelagic clay (Unit 2). This difference in C/N may reflect a difference in composition of the original organic input into the sediment or differences in diagenetic processes. The higher C/N for Unit 1 corresponds to sediments deposited at relatively high sedimentation rates (approx. 130 m/m.y.), whereas the lower C/N for Unit 2 corresponds to sediments deposited at a much lower sedimentation rate.

The carbonate content remains below the detection limit (<0.05% $CaCO_3$) throughout, suggesting deposition below the CCD and/or significant carbonate dissolution (Heath et al., 1977). These results are consistent with sparsity of calcareous fossils. The hydrogen content of the sediments varied from 0.83% to 1.17%. Low C/H (1.9–0.1) indicates that the major portion of the hydrogen detected is related not to the organic matter but to the residual water in minerals not liberated under the drying conditions used for the samples (12 hr. 105°/C).

Conclusions

We detected no evidence of organic gases and/or petroleum-related hydrocarbons at this site, nor did we observe spontaneous release of gas. The only gas detected by forced degasification was CO_2. The sediments have a low to intermediate organic potential, and the organic matter has a low degree of maturation.

PHYSICAL PROPERTIES

Site 487 physical property analyses included porosity, wet bulk density, water content, compressional sound velocity, and undrained shear strength (Fig. 7). These were determined by standard DSDP procedures (Boyce, 1976). Physical properties of these hemipelagic and pelagic sediments display subtle variations with depth. Deviations from this trend are a result not of increased core disturbance but of changes in sedimentation rate and/or lithology.

Porosity, Bulk Density, and Water Content

Porosity and water content trends vary inversely with bulk density. Porosity decreases from 80% near the surface to 75% at 158 meters. Water content increases from 50% at the sea floor to 58% at 12 meters. Below 12 meters water content is constant except for inflections at 103 meters and 134 meters. Bulk density increases from 1.35 Mg/m^3 at 3.3 meters to 1.44 Mg/m^3 at 158 meters.

Compressional Velocity

Velocity increases from 1.45 km/s at 30 meters to a maximum of 1.535 km/s at 102.5 meters. Below this depth velocity remains relatively constant.

Shear Strength

Shear strength remains relatively constant at 15 kPa to a depth of 40 meters (Fig. 7). Values at greater depths scatter, the maximum value exceeding 100 kPa at 112 meters.

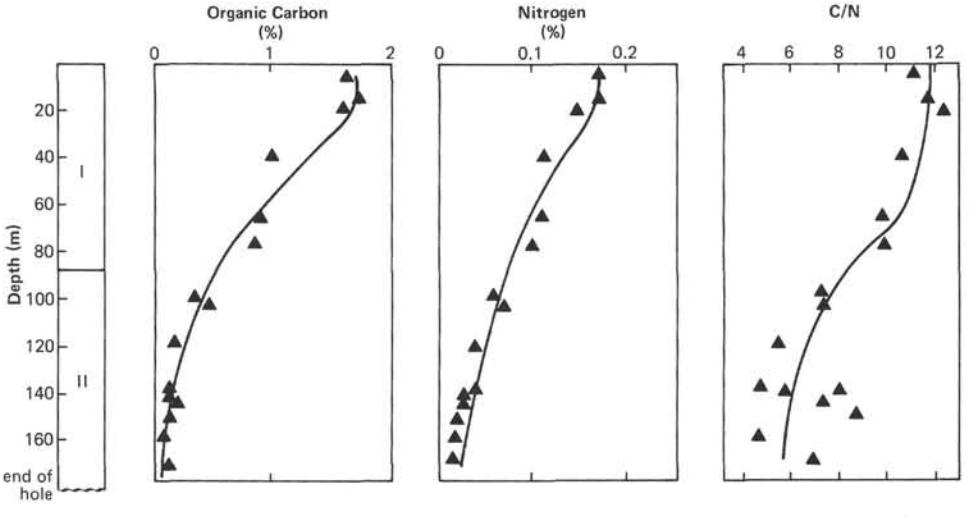

Figure 6. Organic carbon and nitrogen. (See Organic Geochemistry.)

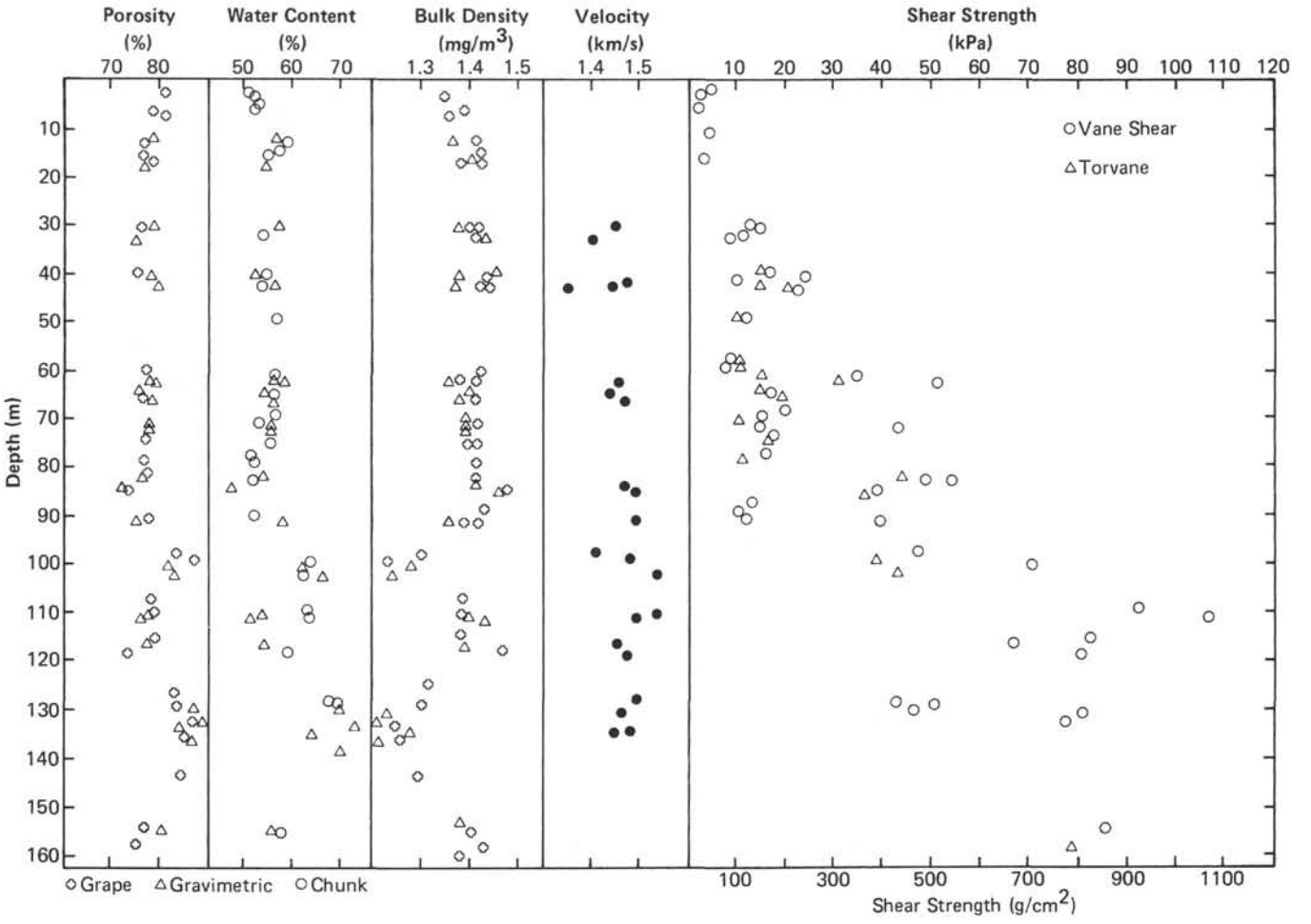

Figure 7. Physical properties summary profiles, Site 487. (See note on figure. This needs additional clarification.)

IGNEOUS PETROGRAPHY

Two meters of basalt fragments were recovered at Site 487. These rocks are principally fine-grained plagioclase–olivine phyric basalt, with minor amounts of aphyric basalt. The basalt is commonly variolitic, and the lowermost fragment we recovered is volcanic glass.

Plagioclase phenocrysts form up to 5% of the basalt and are as large as 4 mm across; olivine phenocrysts are rare, generally less than 1% of the rock, less than 1.5 mm across, and commonly altered to iddingsite and clays. Plagioclase and olivine phenocrysts often form glomeroporphyritic clusters, which are typically somewhat rounded, and plagioclase phenocrysts often contain abundant inclusions of glass blebs and rare euhedral crystals of chrome spinels. The groundmass is typically intersertal. It is composed of 3% to 10% olivine, as euhedral to subhedral crystals, occasionally at the centers of clusters of radiating plagioclase laths; 25% to 40% plagioclase, as euhedral to subhedral laths, acicular needles, and rare skeletal crystals; 20% to 35% clinopyroxene, generally very fine-grained, often forming dendritic intergrowths with fine titanomagnetite dust and minute plagioclase needles but also occasionally as small skeletal crystals; 2% titanomagnetite dust; and 15% to 35% glass, partially altered to palagonite and clays. Vesicles form less than 2% of the basalt and are generally partially filled by clays.

CORRELATION OF SEISMIC REFLECTION AND DRILLING RESULTS

Site 487 lies in a small basin that trends parallel to the trench axis. Seismic reverberations in *Glomar Challenger* reflection data obscure primary sub-bottom reflections (Fig. 8). However, the multichannel seismic reflection profile Line OM-7N, about 1800 meters northwest of the site, shows a single reflection in the middle of the sedimentary section in the center of the basin that rises (within the section) on both the seaward and landward flanks of the basin (Fig. 9).

The prominent reflection within the sedimentary section occurs at about 0.07 s sub-bottom. It may be a receiver ghost effect masking reflections related to the geology. Other, weaker reflections occur at greater depths in the section southwest of the site as projected to this seismic line, but reverberations in the *Challenger* data make correlations impossible. No observed changes in mineralogy, grain size, or diagenesis would significantly affect acoustic impedance. The seismic reflection data thus express the monotonous nature of the drilled

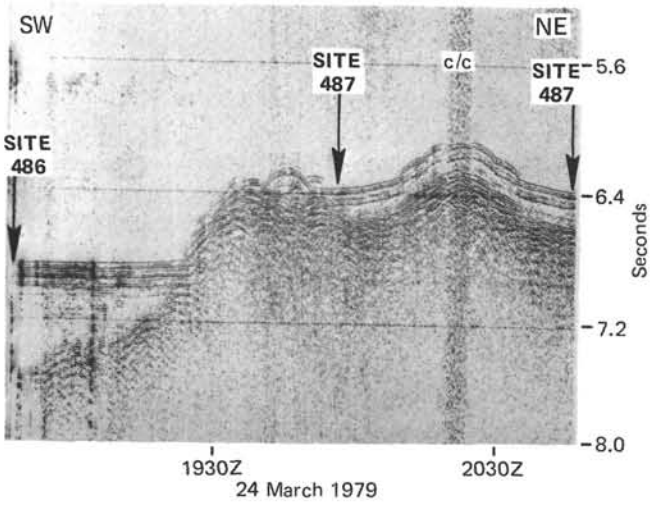

Figure 8. *Glomar Challenger* seismic reflection profile from Site 486 to Site 487. Arrows indicate site location; a course reversal occurred between them.

section, with a possible significant change only in the early Pleistocene.

SUMMARY AND CONCLUSIONS

We achieved the basic objective at Site 487 by penetrating the 171-meter-thick supracrustal sedimentary sequence and bottoming in basalt, presumably oceanic basement. Oldest sediments recovered in Hole 487 were dated as late Miocene, slightly younger than the middle Miocene age attributed to oceanic crust at this location by Lynn and Lewis (1976) on the basis of magnetic anomalies. We regard this age agreement as reasonable, considering the paucity of fauna in the lowermost part of the section and possible errors in locating magnetic stripe boundaries.

The paucity of carbonate microfossil remains suggests that all sediments recovered were deposited below the CCD.

Paleomagnetic polarity reversals were generally consistent with paleontological data and provided a basis for estimating ages in those parts of the sedimentary sequence where paleontological data were missing or nondiagnostic. Hole 487 paleomagnetic measurements show therefore that core orientations at this site were sufficiently stable for meaningful paleomagnetic determinations and that these data can be of significant value in establishing age-depth relationships.

Gases recovered contained no hydrocarbon indicators, nor did we find indications of gas hydrates. Gases consisted of biogenic methane, carbon dioxide, and undetermined nonhydrocarbons.

Sediments in Hole 487 consisted of an upper 105-meter-thick Quaternary unit composed of hemipelagic gray mud and a lower 66-meter-thick upper Miocene–Pliocene unit composed of brown pelagic clay. These units evidence a dramatic change in depositional environment occurring sometime in the late Pliocene or early Quaternary, when the hole location began to accumulate hemipelagic sediments derived from the Mexican margin. Deposition rates of Miocene–Pliocene clays ranged from 29 m/m.y. in the lower part to 7 m/m.y. in the upper part. The decrease in sedimentation rate may reflect more intense solution as the site moved from the crest of the East Pacific Rise to lower elevations on the flank of the rise.

Quaternary mud deposition rates ranged up to 126 m/m.y. These rates reflect increasing proximity of the site to the source of continental hemipelagic sediments. If present convergence rates have persisted unchanged throughout the Quaternary, earliest hemipelagic deposition occurred at a distance of more than 100 km from the trench axis. The transport mechanism of the hemipelagic sediments is uncertain; density currents representing the distal fringes of turbidity flows originating in inner slope submarine canyons may have been responsible. If so, the density currents appear to have climbed at least 1000 meters up the outer slope of the

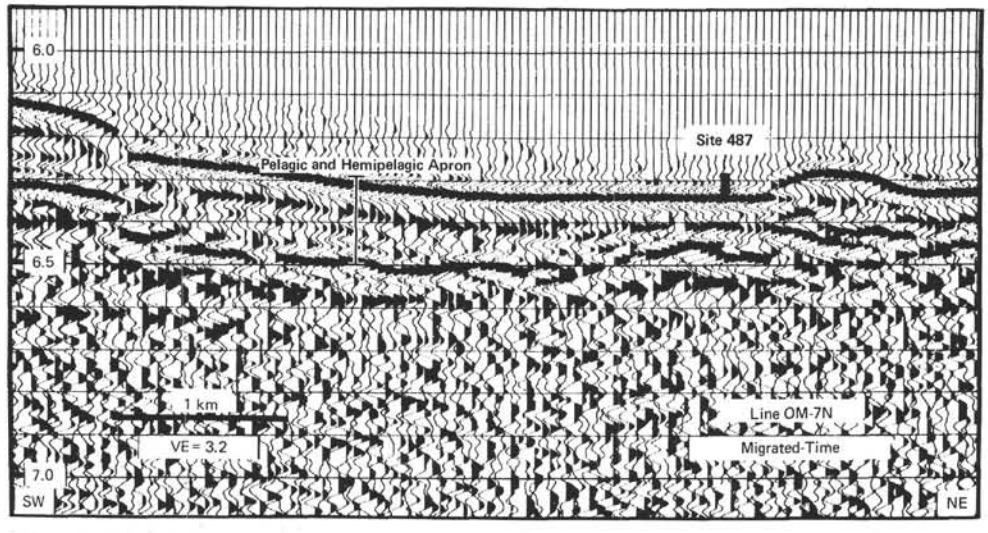

Figure 9. Line 0M-7N seismic profile 1800 meters northwest of Site 487.

trench. Alternatively, portions of the hemipelagic sediments may have accumulated from grain-by-grain settling through the water column.

REFERENCES

Berggren, W. A., and Van Couvering, J. A., 1974. *The Late Neogene:* Amsterdam (Elsevier), p. 216.

Boyce, R. E., 1976. Definitions and laboratory techniques of compressional sound velocity parameters and wet water content, wet bulk density and porosity parameters by gravimetric and gamma ray attenuation techniques. *In* Schlanger, S. O., Jackson, E. D., et al., *Init. Repts. DSDP*, 33: Washington (U.S. Govt. Printing Office), 931–958.

Bukry, D., 1973. Low-latitude coccolith biostratigraphic zonation. *In* Edgar, N. T., Saunders, J. B., et al., *Init. Repts. DSDP*, 15: Washington (U.S. Govt. Printing Office), 715–735.

Dinkelman, M. G., 1973. Radiolarian stratigraphy: Leg 16, Deep Sea Drilling Project. *In* van Andel, Tj. H., Heath, G. R., et al., *Init. Repts. DSDP*, 16: Washington (U.S. Govt. Printing Office), 747–813.

Fairbridge, R. W., 1972. *The Encyclopedia of Geochemistry and Environmental Sciences:* New York (Van Nostrand), pp. 136–141.

Hays, J. D., 1970. Stratigraphy and evolutionary trends in North Pacific deep-sea sediments. *Geol. Soc. Am. Mem. 126*, 185–218.

Heath, G. R., Moore, T. C., Jr., and van Andel, Tj. H., 1977. Carbonate accumulation and dissolution in the equatorial Pacific during the past 45 million years. *In* Andersen, N. R., and Malahoff, A. (Eds.), *The Fate of Fossil Fuel CO_2 in the Oceans:* New York (Plenum Press), pp. 627–639.

Karig, D. E., Cardwell, R. F., Moore, G. F., et al., 1978. Late Cenozoic subduction and continental margin truncation along the northern Middle American Trench. *Geol. Soc. Am. Bull.*, 89: 265–276.

Lynn, W. A., and Lewis, B. T. R., 1976. Tectonic evolution of the northern Cocos Plate. *Geology*, 4:718–722.

Martini, E., 1971. Standard Tertiary and Quaternary calcareous nannoplankton zonation. *In* Farinacci, A. (Ed.), *Proc. Second Plankt. Conf., Roma, 1970*, 2: Rome (Edizeoni Tecno-Scienza), 739–785.

Minister, J. B., and Jordan, T. H., 1978. Present-day plate motions. *J. Geophys. Res.*, 83:5331–5354.

Nigrini, C., 1971. Radiolarian zones in the Quaternary of the equatorial Pacific Ocean. *In* Funnell, B. M., and Riedel, W. R. (Eds.), *The Micropaleontology of Oceans:* Cambridge (Cambridge University Press), pp. 443–461.

Riedel, W. R., and Sanfilippo, A., 1971. Cenozoic radiolaria from the western tropical Pacific, Leg 7. *In* Winterer, E. L., Riedel, W. R., et al., *Init. Repts. DSDP*, 7, Pt. 2: Washington (U.S. Govt. Printing Office), 1529–1672.

Ryan, W. B. F., Cita, M. B., Rowson, M. D., et al., 1974. A paleomagnetic assignment to Neogene stage boundaries and the development of isochronous datum planes between the Mediterranean, the Pacific and Indian Oceans in order to investigate the response of the world ocean of the Mediterranean "salinity crisis." *Riv. Ital. Pal.*, 80:631–638.

Tardy, M., 1977. Essai sur la reconstruction de l'évolution paléogéographique et structurale de la partie septentrionale du Mexique au cours du Mésozoïque et du Cénozoïque. *Bull. Soc. Geol. France*, (7)4.19 (no. 6):1297–1308.

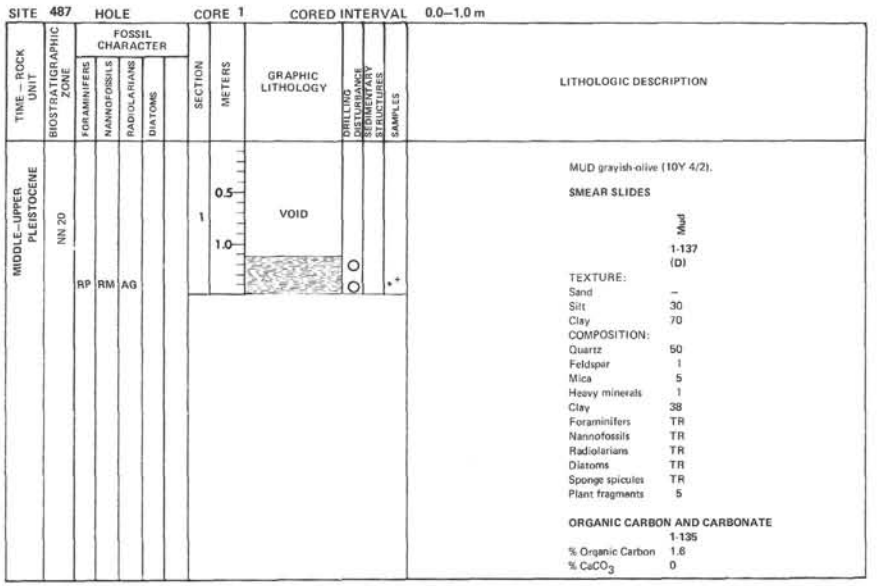
SITE 487 HOLE CORE 1 CORED INTERVAL 0.0–1.0 m
TIME – ROCK UNIT
BIOSTRATIGRAPHIC ZONE
FOSSIL CHARACTER
FORAMINIFERS
NANNOFOSSILS
RADIOLARIANS
DIATOMS
SECTION
METERS
GRAPHIC LITHOLOGY
DRILLING DISTURBANCE
SEDIMENTARY STRUCTURES
SAMPLES
LITHOLOGIC DESCRIPTION
MIDDLE–UPPER PLEISTOCENE
NN 20
RP RM AG
1
0.5
1.0
VOID
MUD grayish-olive (10Y 4/2).
SMEAR SLIDES
Mud
1-137 (D)
TEXTURE:
Sand –
Silt 30
Clay 70
COMPOSITION:
Quartz 50
Feldspar 1
Mica 5
Heavy minerals 1
Clay 38
Foraminifers TR
Nannofossils TR
Radiolarians TR
Diatoms TR
Sponge spicules TR
Plant fragments 5
ORGANIC CARBON AND CARBONATE
1-135
% Organic Carbon 1.8
% CaCO3 0

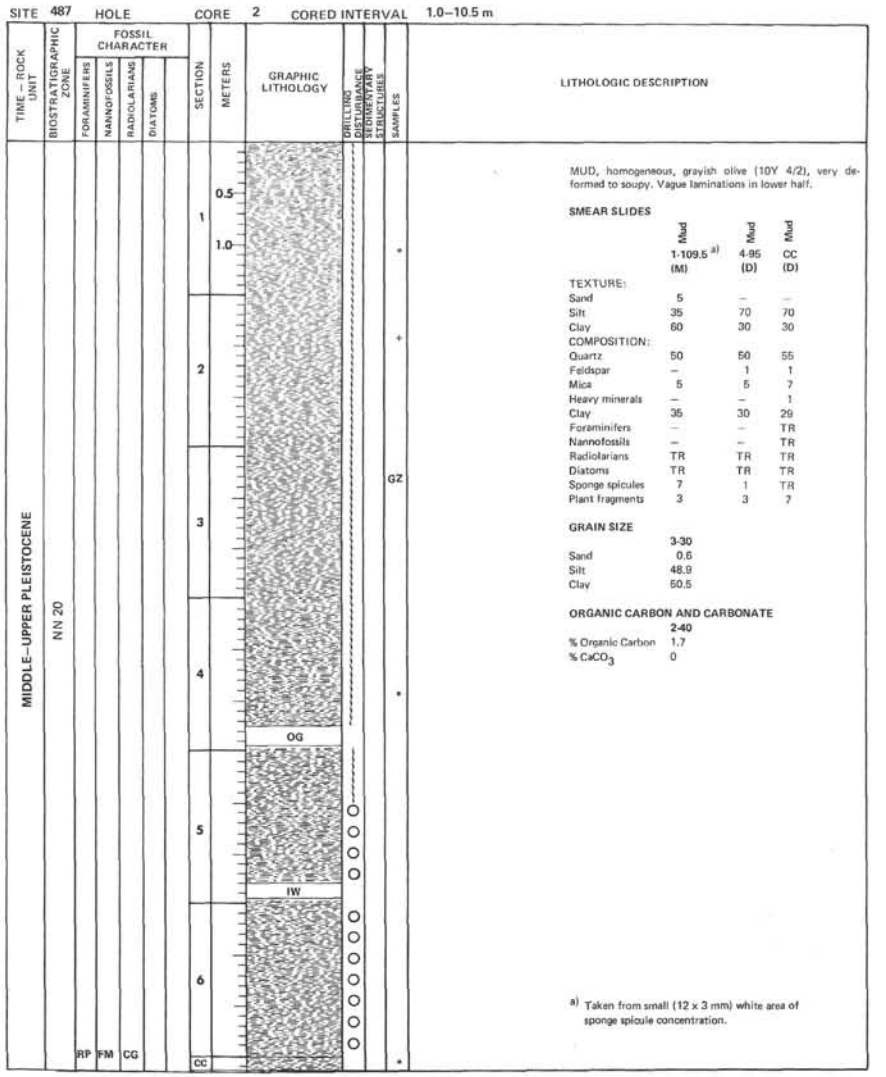
SITE 487 HOLE CORE 2 CORED INTERVAL 1.0–10.5 m
TIME – ROCK UNIT
BIOSTRATIGRAPHIC ZONE
FOSSIL CHARACTER
FORAMINIFERS
NANNOFOSSILS
RADIOLARIANS
DIATOMS
SECTION
METERS
GRAPHIC LITHOLOGY
DRILLING DISTURBANCE
SEDIMENTARY STRUCTURES
SAMPLES
LITHOLOGIC DESCRIPTION
MIDDLE–UPPER PLEISTOCENE
NN 20
RP FM CG
1
2
3
4
5
6
CC
0.5
1.0
OG
IW
GZ
MUD, homogeneous, grayish olive (10Y 4/2), very deformed to soupy. Vague laminations in lower half.
SMEAR SLIDES
Mud 1-109.5 a) (M)
Mud 4-95 (D)
Mud CC (D)
TEXTURE:
Sand 5 – –
Silt 35 70 70
Clay 60 30 30
COMPOSITION:
Quartz 50 60 55
Feldspar – 1 1
Mica 5 5 7
Heavy minerals – – 1
Clay 35 30 29
Foraminifers – – TR
Nannofossils – – TR
Radiolarians TR TR TR
Diatoms TR TR TR
Sponge spicules 7 1 TR
Plant fragments 3 3 7
GRAIN SIZE
3-30
Sand 0.6
Silt 48.9
Clay 50.5
ORGANIC CARBON AND CARBONATE
2-40
% Organic Carbon 1.7
% CaCO3 0
a) Taken from small (12 x 3 mm) white area of sponge spicule concentration.

SITE 487 HOLE CORE 3 CORED INTERVAL 10.5–20.0 m

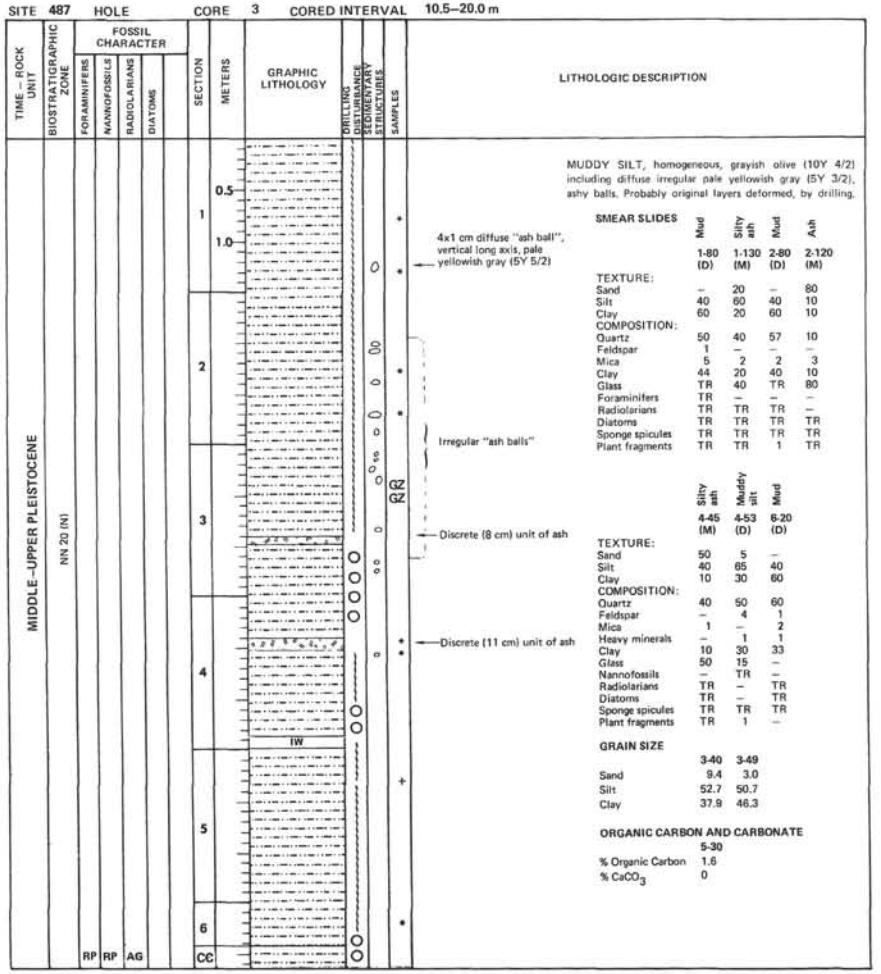

MUDDY SILT, homogeneous, grayish olive (10Y 4/2) including diffuse irregular pale yellowish gray (5Y 3/2), ashy balls. Probably original layers deformed, by drilling.

SMEAR SLIDES

	Mud	Silty ash	Mud	Ash
	1-80 (D)	1-130 (M)	2-80 (D)	2-120 (M)
TEXTURE:				
Sand	–	20	–	80
Silt	40	60	40	10
Clay	60	20	60	10
COMPOSITION:				
Quartz	50	40	57	10
Feldspar	1	–	–	–
Mica	5	2	2	3
Clay	44	20	40	10
Glass	TR	40	TR	80
Foraminifers	TR	–	–	–
Radiolarians	TR	TR	TR	–
Diatoms	TR	TR	TR	TR
Sponge spicules	TR	TR	TR	TR
Plant fragments	TR	TR	1	TR

	Silty ash	Muddy silt	Mud
	4-45 (M)	4-53 (D)	6-20 (D)
TEXTURE:			
Sand	50	5	–
Silt	40	65	40
Clay	10	30	60
COMPOSITION:			
Quartz	40	50	60
Feldspar	–	4	1
Mica	1	–	2
Heavy minerals	–	1	1
Clay	10	30	33
Glass	50	15	–
Nannofossils	–	TR	–
Radiolarians	TR	–	TR
Diatoms	TR	–	TR
Sponge spicules	TR	TR	TR
Plant fragments	TR	1	–

GRAIN SIZE

	3-40	3-49
Sand	9.4	3.0
Silt	52.7	50.7
Clay	37.9	46.3

ORGANIC CARBON AND CARBONATE

	5-30
% Organic Carbon	1.6
% $CaCO_3$	0

SITE 487 HOLE CORE 4 CORED INTERVAL 20.0–29.5 m

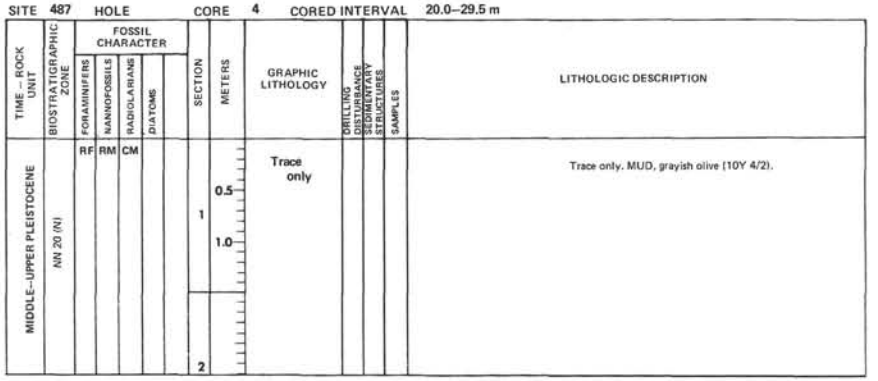

Trace only. MUD, grayish olive (10Y 4/2).

SITE 487 HOLE CORE 5 CORED INTERVAL 29.5–39.0 m

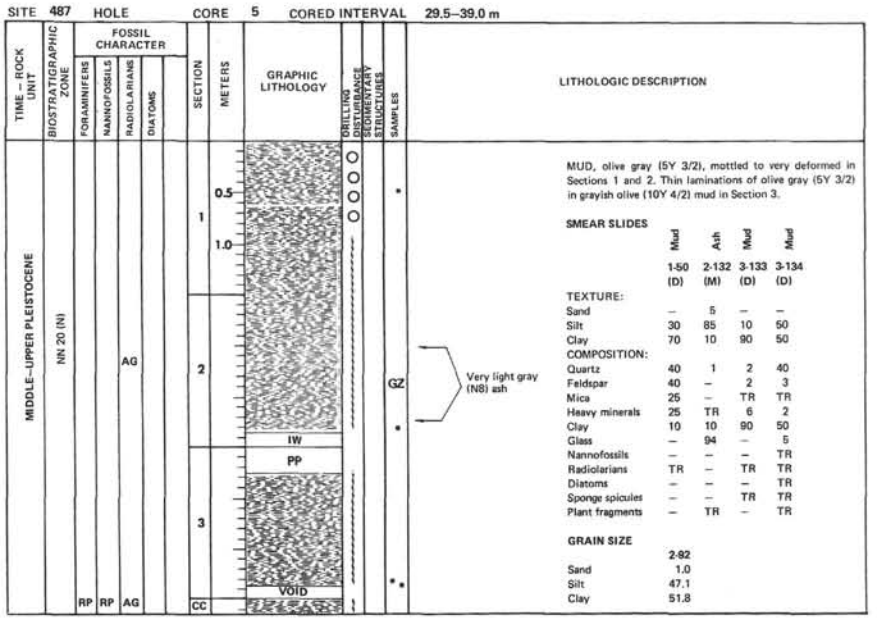

MUD, olive gray (5Y 3/2), mottled to very deformed in Sections 1 and 2. Thin laminations of olive gray (5Y 3/2) in grayish olive (10Y 4/2) mud in Section 3.

SMEAR SLIDES

	Mud	Ash	Mud	Mud
	1-50 (D)	2-132 (M)	3-133 (D)	3-134 (D)
TEXTURE:				
Sand	–	5	–	–
Silt	30	85	10	50
Clay	70	10	90	50
COMPOSITION:				
Quartz	40	1	2	40
Feldspar	40	–	2	3
Mica	25	–	TR	TR
Heavy minerals	25	TR	6	2
Clay	10	10	90	50
Glass	–	94	–	5
Nannofossils	–	–	–	TR
Radiolarians	TR	–	TR	TR
Diatoms	–	–	–	TR
Sponge spicules	–	–	TR	TR
Plant fragments	–	TR	–	TR

GRAIN SIZE

	2-82
Sand	1.0
Silt	47.1
Clay	51.8

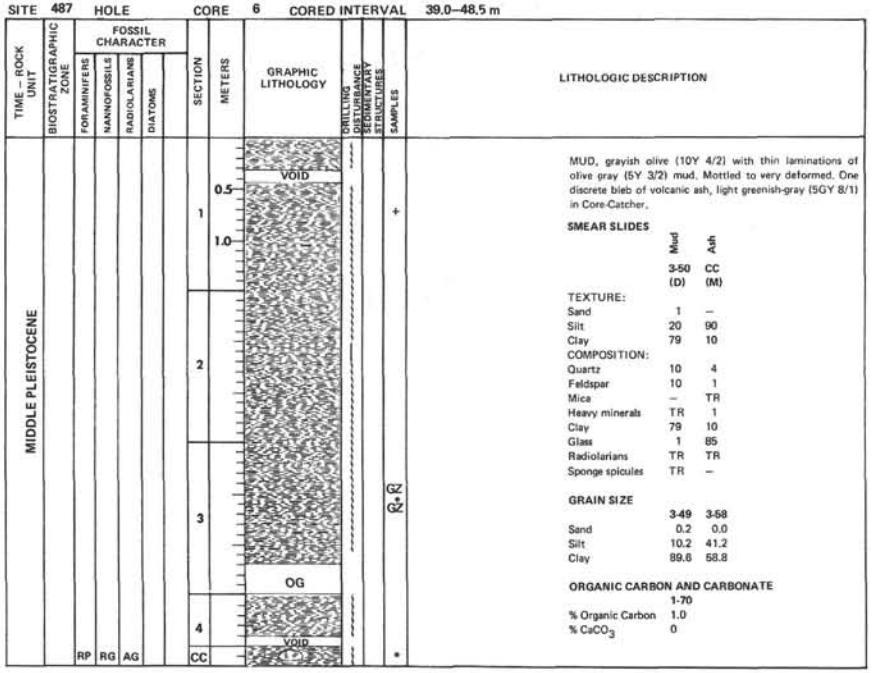
SITE 487 HOLE CORE 6 CORED INTERVAL 39.0–48.5 m
TIME – ROCK UNIT
BIOSTRATIGRAPHIC ZONE
FOSSIL CHARACTER
FORAMINIFERS
NANNOFOSSILS
RADIOLARIANS
DIATOMS
SECTION
METERS
GRAPHIC LITHOLOGY
DRILLING DISTURBANCE
SEDIMENTARY STRUCTURES
SAMPLES
LITHOLOGIC DESCRIPTION
MIDDLE PLEISTOCENE
RP RG AG
VOID
OG
VOID
MUD, grayish olive (10Y 4/2) with thin laminations of olive gray (5Y 3/2) mud. Mottled to very deformed. One discrete bleb of volcanic ash, light greenish-gray (5GY 8/1) in Core-Catcher.
SMEAR SLIDES
Mud 3-50 (D)
Ash CC (M)
TEXTURE:
Sand 1 –
Silt 20 90
Clay 79 10
COMPOSITION:
Quartz 10 4
Feldspar 10 1
Mica – TR
Heavy minerals TR 1
Clay 79 10
Glass 1 85
Radiolarians TR TR
Sponge spicules TR –
GRAIN SIZE
3-49 3-58
Sand 0.2 0.0
Silt 10.2 41.2
Clay 89.6 58.8
ORGANIC CARBON AND CARBONATE
1-70
% Organic Carbon 1.0
% CaCO3 0

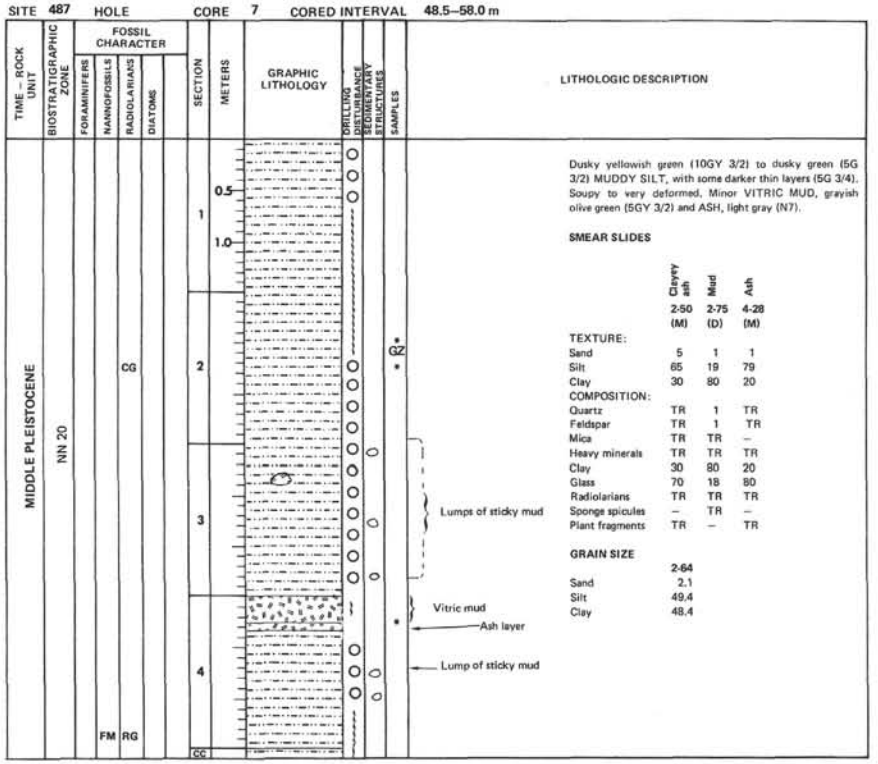
SITE 487 HOLE CORE 7 CORED INTERVAL 48.5–58.0 m
TIME – ROCK UNIT
BIOSTRATIGRAPHIC ZONE
FOSSIL CHARACTER
FORAMINIFERS
NANNOFOSSILS
RADIOLARIANS
DIATOMS
SECTION
METERS
GRAPHIC LITHOLOGY
DRILLING DISTURBANCE
SEDIMENTARY STRUCTURES
SAMPLES
LITHOLOGIC DESCRIPTION
MIDDLE PLEISTOCENE
NN 20
CG
FM RG
Lumps of sticky mud
Vitric mud
Ash layer
Lump of sticky mud
Dusky yellowish green (10GY 3/2) to dusky green (5G 3/2) MUDDY SILT, with some darker thin layers (5G 3/4). Soupy to very deformed. Minor VITRIC MUD, grayish olive green (5GY 3/2) and ASH, light gray (N7).
SMEAR SLIDES
Clayey ash 2-50 (M)
Mud 2-75 (D)
Ash 4-28 (M)
TEXTURE:
Sand 5 1 1
Silt 65 19 79
Clay 30 80 20
COMPOSITION:
Quartz TR 1 TR
Feldspar TR 1 TR
Mica TR TR –
Heavy minerals TR TR TR
Clay 30 80 20
Glass 70 18 80
Radiolarians TR TR TR
Sponge spicules – TR –
Plant fragments TR – TR
GRAIN SIZE
2-64
Sand 2.1
Silt 49.4
Clay 48.4

SITE 487 HOLE CORE 8 CORED INTERVAL 58.0–67.5 m

TIME – ROCK UNIT	BIOSTRATIGRAPHIC ZONE	FOSSIL CHARACTER: FORAMINIFERS	NANNOFOSSILS	RADIOLARIANS	DIATOMS	SECTION	METERS	GRAPHIC LITHOLOGY	DRILLING DISTURBANCE	SEDIMENTARY STRUCTURES	SAMPLES	LITHOLOGIC DESCRIPTION
LOWER–MIDDLE PLEISTOCENE	NN 19 (N)	FM	FM	RG		1	0.5					Shell fragment (plate of sea urchin?)
				FM		1	1.0					MUD, dusky yellowish green (10GY 3/2) to grayish olive green (5GY 3/2). Very deformed thin laminations.
						2						SMEAR SLIDES
						3					GZ	Ash fragment
						4						Organic material or sulfide fragment; Discontinuous ash bed
						5		IW PP				
						6						Ash fragment
						CC						

SMEAR SLIDES	Mud 3-50 (D)
TEXTURE:	
Sand	–
Silt	20
Clay	80
COMPOSITION:	
Quartz	15
Feldspar	2
Mica	TR
Heavy minerals	TR
Clay	80
Glass	2
Radiolarians	2
Diatoms	TR
Sponge spicules	TR
Pyrite	1
GRAIN SIZE	
Sand	0.2
Silt	43.3
Clay	56.5
ORGANIC CARBON AND CARBONATE	5-136
% Organic Carbon	0.9
% $CaCO_3$	0

SITE 487 HOLE CORE 9 CORED INTERVAL 67.5–77.0 m

TIME – ROCK UNIT	BIOSTRATIGRAPHIC ZONE	FOSSIL CHARACTER: FORAMINIFERS	NANNOFOSSILS	RADIOLARIANS	DIATOMS	SECTION	METERS	GRAPHIC LITHOLOGY	DRILLING DISTURBANCE	SEDIMENTARY STRUCTURES	SAMPLES	LITHOLOGIC DESCRIPTION
LOWER–MIDDLE PLEISTOCENE	NN 19 (N)	RP	RP	FM		1	0.5					MUD, grayish olive green (5GY 3/2) moderately mottled to very deformed and olive gray (5Y 3/2) to olive black (5Y 2/1) mud beginning in Section 4.
						1	1.0					SMEAR SLIDES
						2					GZ	Grayish olive green; Olive gray to olive black
						3						
						4						
						5		PP			GZ	Possible bioturbation, extensive mottling of mud almost all 5GY 4/1
						6						
						CC	7	OG				

SMEAR SLIDES	Mud 3-13 (D)	Mud 7-20 (D)
TEXTURE:		
Sand	–	–
Silt	15	35
Clay	85	65
COMPOSITION:		
Quartz	10	25
Feldspar	3	5
Mica	TR	TR
Heavy minerals	–	TR
Clay	85	64
Glass	2	2
Foraminifers	–	TR
Nannofossils	–	1
Radiolarians	TR	1
Diatoms	TR	TR
Sponge spicules	–	1
Pyrite	TR	1
GRAIN SIZE	2-98	5-36
Sand	0.1	0.1
Silt	37.3	41.5
Clay	62.7	58.3

SITE 487 HOLE CORE 10 CORED INTERVAL 77.0–86.5 m

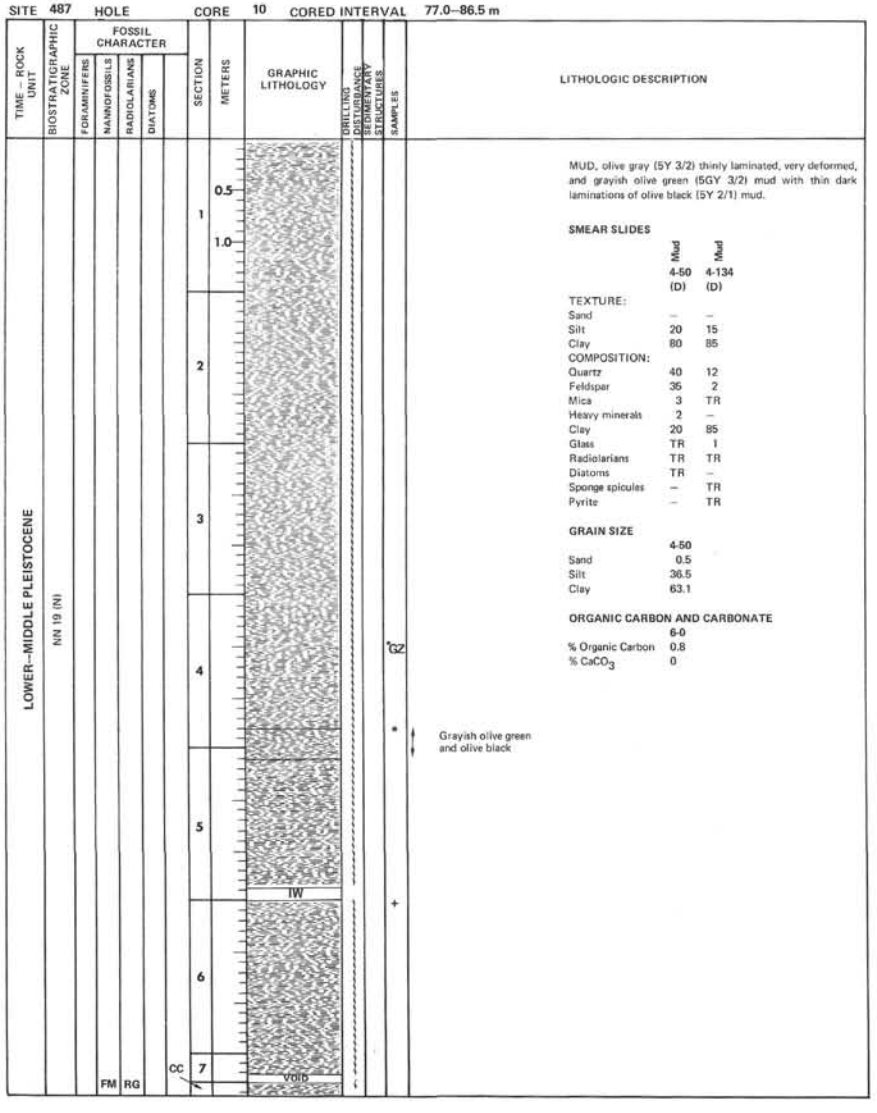

MUD, olive gray (5Y 3/2) thinly laminated, very deformed, and grayish olive green (5GY 3/2) mud with thin dark laminations of olive black (5Y 2/1) mud.

SMEAR SLIDES

	Mud 4-50 (D)	Mud 4-134 (D)
TEXTURE:		
Sand	–	–
Silt	20	15
Clay	80	85
COMPOSITION:		
Quartz	40	12
Feldspar	35	2
Mica	3	TR
Heavy minerals	2	–
Clay	20	85
Glass	TR	1
Radiolarians	TR	TR
Diatoms	TR	–
Sponge spicules	–	TR
Pyrite	–	TR

GRAIN SIZE

	4-50
Sand	0.5
Silt	36.5
Clay	63.1

ORGANIC CARBON AND CARBONATE

	6-0
% Organic Carbon	0.8
% $CaCO_3$	0

SITE 487 HOLE CORE 11 CORED INTERVAL 86.5–96.0 m

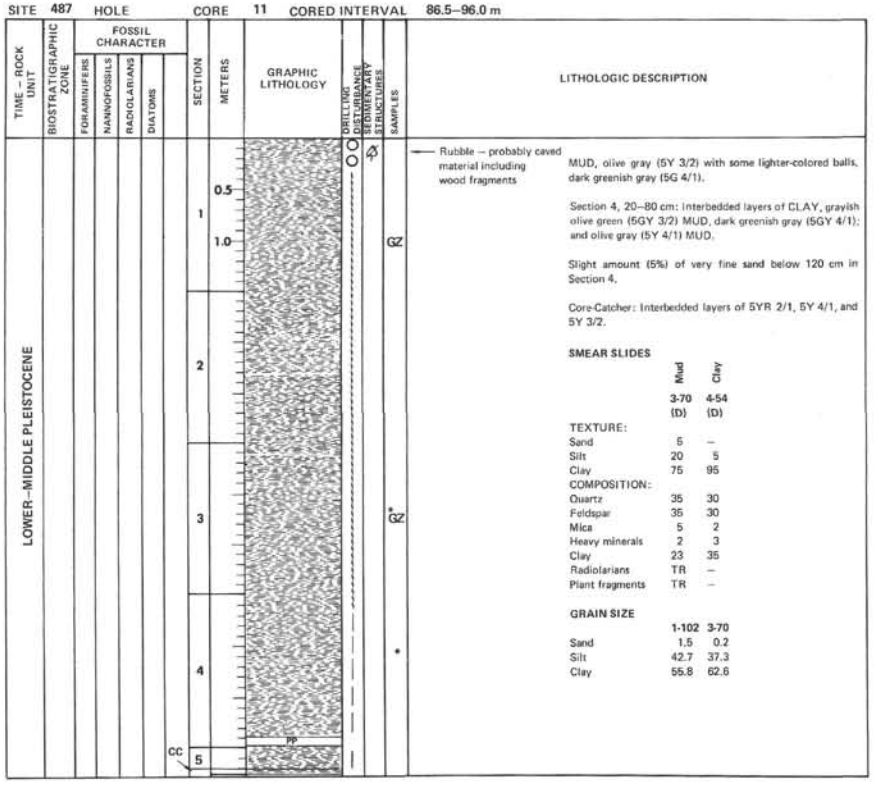

Rubble – probably caved material including wood fragments

MUD, olive gray (5Y 3/2) with some lighter-colored balls, dark greenish gray (5G 4/1).

Section 4, 20–80 cm: interbedded layers of CLAY, grayish olive green (5GY 3/2) MUD, dark greenish gray (5GY 4/1); and olive gray (5Y 4/1) MUD.

Slight amount (5%) of very fine sand below 120 cm in Section 4.

Core-Catcher: Interbedded layers of 5YR 2/1, 5Y 4/1, and 5Y 3/2.

SMEAR SLIDES

	Mud 3-70 (D)	Clay 4-54 (D)
TEXTURE:		
Sand	5	–
Silt	20	5
Clay	75	95
COMPOSITION:		
Quartz	35	30
Feldspar	35	30
Mica	5	2
Heavy minerals	2	3
Clay	23	35
Radiolarians	TR	–
Plant fragments	TR	–

GRAIN SIZE

	1-102	3-70
Sand	1.5	0.2
Silt	42.7	37.3
Clay	55.8	62.6

SITE 487 HOLE CORE 12 CORED INTERVAL 96.0–105.5 m

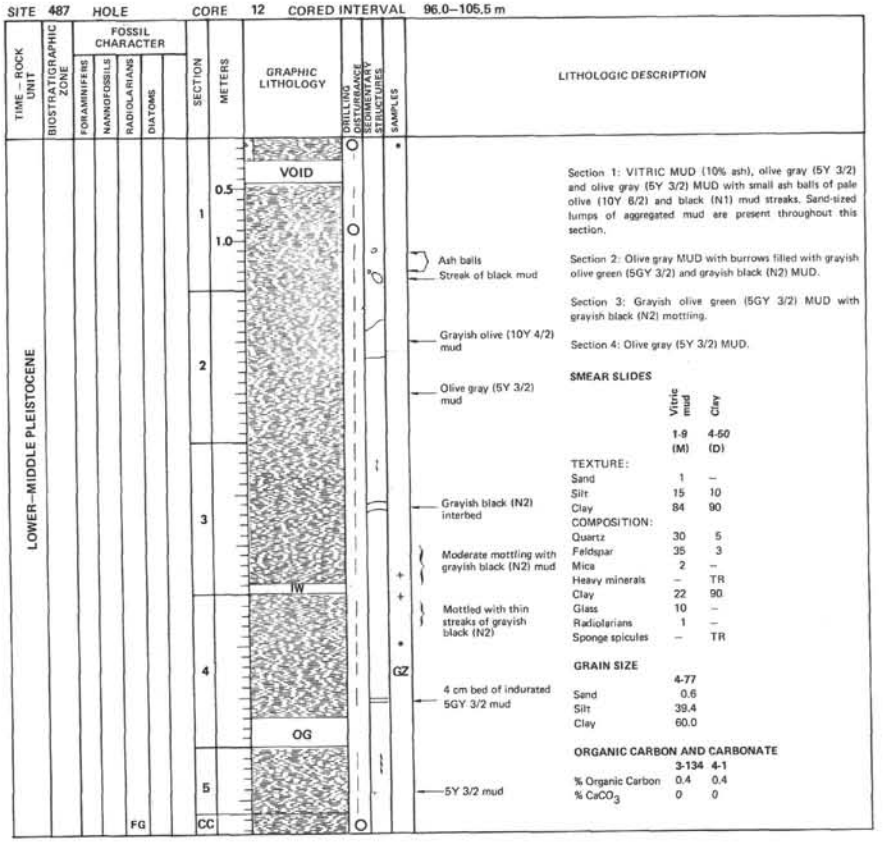

Section 1: VITRIC MUD (10% ash), olive gray (5Y 3/2) and olive gray (5Y 3/2) MUD with small ash balls of pale olive (10Y 6/2) and black (N1) mud streaks. Sand-sized lumps of aggregated mud are present throughout this section.

Section 2: Olive gray MUD with burrows filled with grayish olive green (5GY 3/2) and grayish black (N2) MUD.

Section 3: Grayish olive green (5GY 3/2) MUD with grayish black (N2) mottling.

Section 4: Olive gray (5Y 3/2) MUD.

SMEAR SLIDES

	Vitric mud 1-9 (M)	Clay 4-50 (D)
TEXTURE:		
Sand	1	–
Silt	15	10
Clay	84	90
COMPOSITION:		
Quartz	30	5
Feldspar	35	3
Mica	2	–
Heavy minerals	–	TR
Clay	22	90
Glass	10	–
Radiolarians	1	–
Sponge spicules	–	TR

GRAIN SIZE

	4-77
Sand	0.6
Silt	39.4
Clay	60.0

ORGANIC CARBON AND CARBONATE

	3-134	4-1
% Organic Carbon	0.4	0.4
% $CaCO_3$	0	0

SITE 487 HOLE CORE 13 CORED INTERVAL 105.5–115.0 m

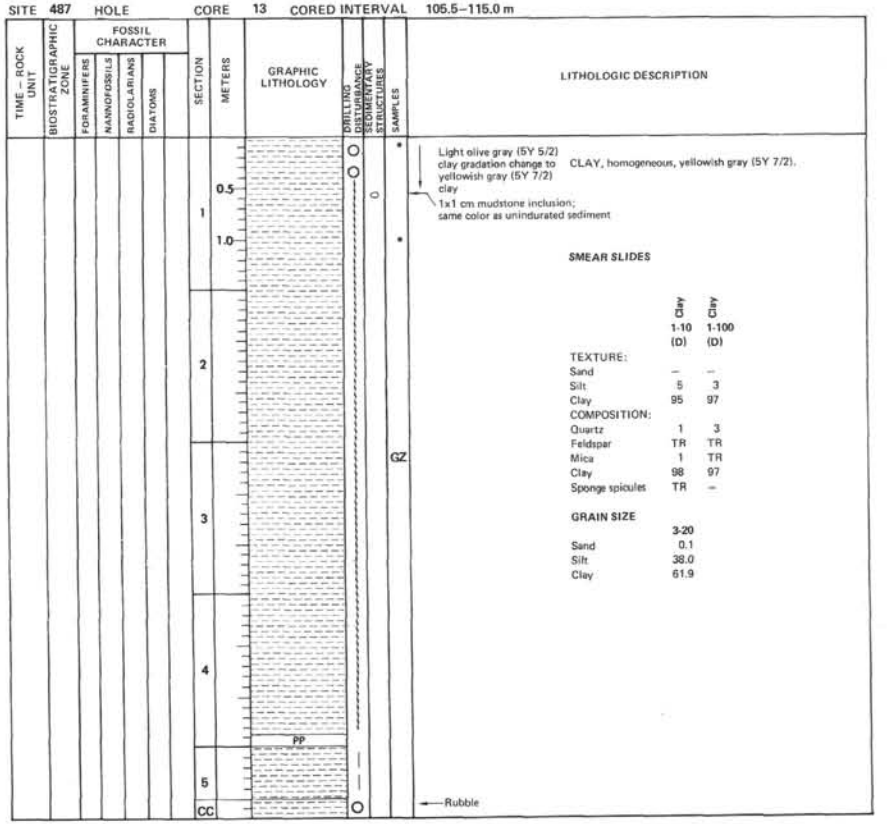

CLAY, homogeneous, yellowish gray (5Y 7/2).

SMEAR SLIDES

	Clay 1-10 (D)	Clay 1-100 (D)
TEXTURE:		
Sand	–	–
Silt	5	3
Clay	95	97
COMPOSITION:		
Quartz	1	3
Feldspar	TR	TR
Mica	1	TR
Clay	98	97
Sponge spicules	TR	–

GRAIN SIZE

	3-20
Sand	0.1
Silt	38.0
Clay	61.9

SITE 487 HOLE CORE 14 CORED INTERVAL 115.0–124.5 m

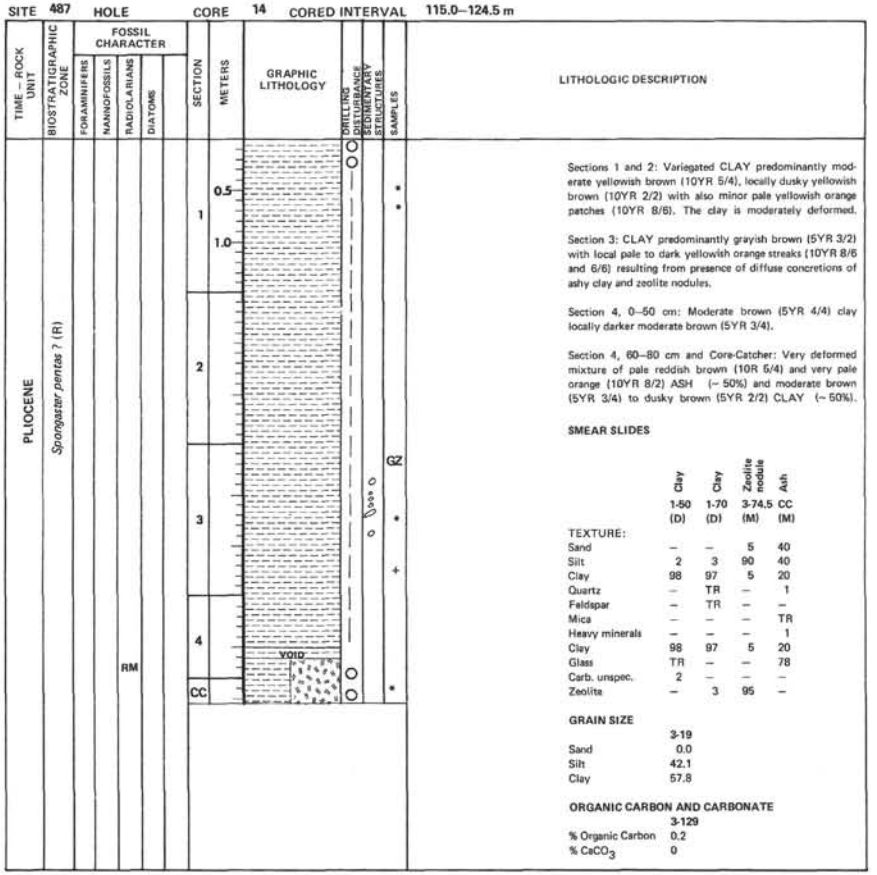

LITHOLOGIC DESCRIPTION

Sections 1 and 2: Variegated CLAY predominantly moderate yellowish brown (10YR 5/4), locally dusky yellowish brown (10YR 2/2) with also minor pale yellowish orange patches (10YR 8/6). The clay is moderately deformed.

Section 3: CLAY predominantly grayish brown (5YR 3/2) with local pale to dark yellowish orange streaks (10YR 8/6 and 6/6) resulting from presence of diffuse concretions of ashy clay and zeolite nodules.

Section 4, 0–50 cm: Moderate brown (5YR 4/4) clay locally darker moderate brown (5YR 3/4).

Section 4, 60–80 cm and Core-Catcher: Very deformed mixture of pale reddish brown (10R 5/4) and very pale orange (10YR 8/2) ASH (~ 50%) and moderate brown (5YR 3/4) to dusky brown (5YR 2/2) CLAY (~ 50%).

SMEAR SLIDES

	Clay 1-50 (D)	Clay 1-70 (D)	Zeolite nodule 3-74.5 (M)	Ash CC (M)
TEXTURE:				
Sand	–	–	5	40
Silt	2	3	90	40
Clay	98	97	5	20
Quartz	–	TR	–	1
Feldspar	–	TR	–	–
Mica	–	–	–	TR
Heavy minerals	–	–	–	1
Clay	98	97	5	20
Glass	TR	–	–	78
Carb. unspec.	2	–	–	–
Zeolite	–	3	95	–

GRAIN SIZE

	3-19
Sand	0.0
Silt	42.1
Clay	57.8

ORGANIC CARBON AND CARBONATE

	3-129
% Organic Carbon	0.2
% $CaCO_3$	0

SITE 487 HOLE CORE 15 CORED INTERVAL 124.5–134.0 m

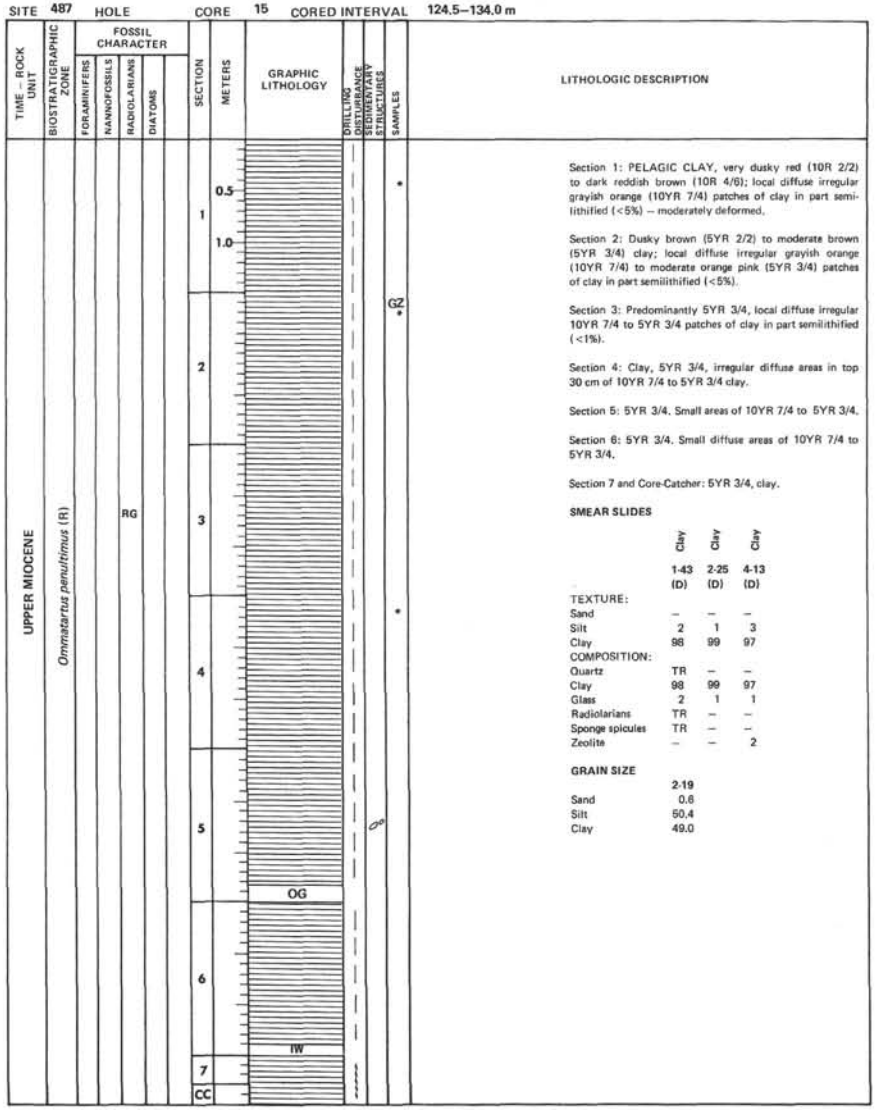

LITHOLOGIC DESCRIPTION

Section 1: PELAGIC CLAY, very dusky red (10R 2/2) to dark reddish brown (10R 4/6); local diffuse irregular grayish orange (10YR 7/4) patches of clay in part semilithified (<5%) – moderately deformed.

Section 2: Dusky brown (5YR 2/2) to moderate brown (5YR 3/4) clay; local diffuse irregular grayish orange (10YR 7/4) to moderate orange pink (5YR 3/4) patches of clay in part semilithified (<5%).

Section 3: Predominantly 5YR 3/4, local diffuse irregular 10YR 7/4 to 5YR 3/4 patches of clay in part semilithified (<1%).

Section 4: Clay, 5YR 3/4, irregular diffuse areas in top 30 cm of 10YR 7/4 to 5YR 3/4 clay.

Section 5: 5YR 3/4. Small areas of 10YR 7/4 to 5YR 3/4.

Section 6: 5YR 3/4. Small diffuse areas of 10YR 7/4 to 5YR 3/4.

Section 7 and Core-Catcher: 5YR 3/4, clay.

SMEAR SLIDES

	Clay 1-43 (D)	Clay 2-25 (D)	Clay 4-13 (D)
TEXTURE:			
Sand	–	–	–
Silt	2	1	3
Clay	98	99	97
COMPOSITION:			
Quartz	TR	–	–
Clay	98	99	97
Glass	2	1	1
Radiolarians	TR	–	–
Sponge spicules	TR	–	–
Zeolite	–	–	2

GRAIN SIZE

	2-19
Sand	0.6
Silt	50.4
Clay	49.0

SITE 487 HOLE CORE 16 CORED INTERVAL 134.0–143.5 m

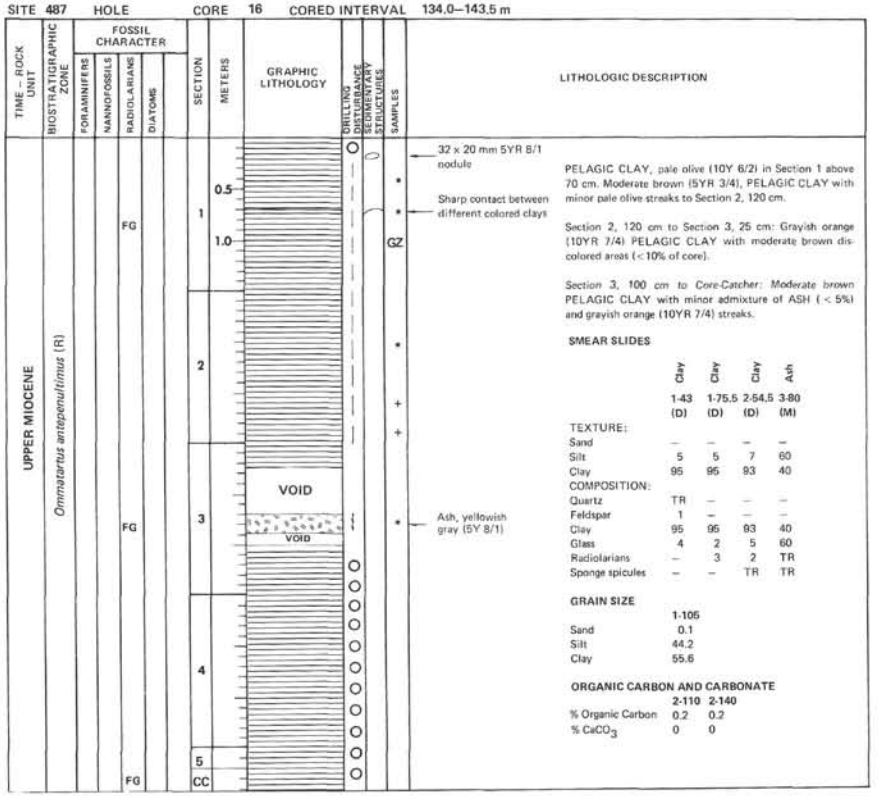

PELAGIC CLAY, pale olive (10Y 6/2) in Section 1 above 70 cm. Moderate brown (5YR 3/4), PELAGIC CLAY with minor pale olive streaks to Section 2, 120 cm.

Section 2, 120 cm to Section 3, 25 cm: Grayish orange (10YR 7/4) PELAGIC CLAY with moderate brown discolored areas (< 10% of core).

Section 3, 100 cm to Core-Catcher: Moderate brown PELAGIC CLAY with minor admixture of ASH (< 5%) and grayish orange (10YR 7/4) streaks.

SMEAR SLIDES

	Clay 1-43 (D)	Clay 1-75.5 (D)	Clay 2-54.5 (D)	Ash 3-80 (M)
TEXTURE:				
Sand	–	–	–	–
Silt	5	5	7	60
Clay	95	95	93	40
COMPOSITION:				
Quartz	TR	–	–	–
Feldspar	1	–	–	–
Clay	95	95	93	40
Glass	4	2	5	60
Radiolarians	–	3	2	TR
Sponge spicules	–	–	TR	TR

GRAIN SIZE

	1-105
Sand	0.1
Silt	44.2
Clay	55.6

ORGANIC CARBON AND CARBONATE

	2-110	2-140
% Organic Carbon	0.2	0.2
% $CaCO_3$	0	0

SITE 487 HOLE CORE 17 CORED INTERVAL 143.5–153.0 m

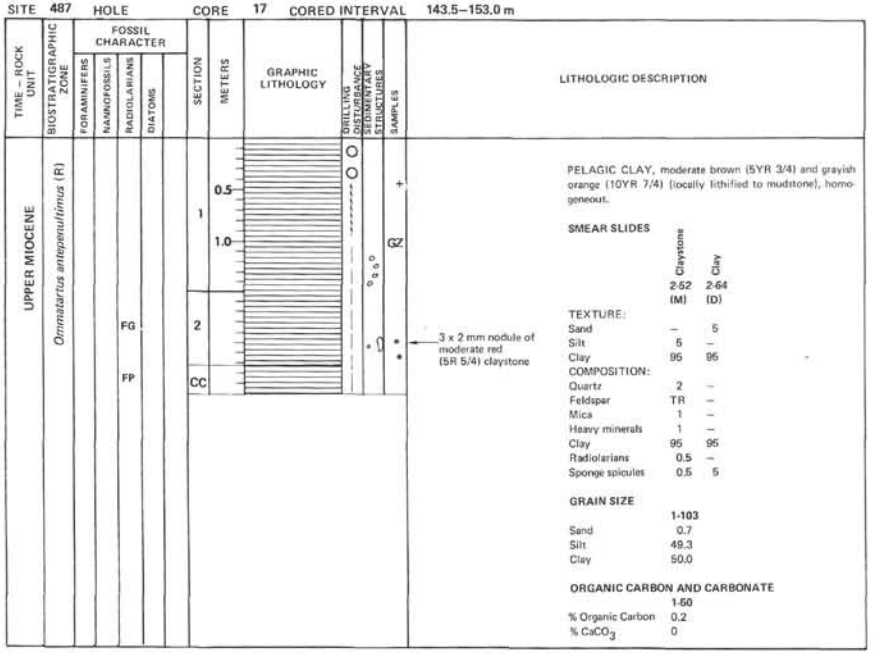

PELAGIC CLAY, moderate brown (5YR 3/4) and grayish orange (10YR 7/4) (locally lithified to mudstone), homogeneous.

SMEAR SLIDES

	Claystone 2-52 (M)	Clay 2-64 (D)
TEXTURE:		
Sand	–	5
Silt	5	–
Clay	95	95
COMPOSITION:		
Quartz	2	–
Feldspar	TR	–
Mica	1	–
Heavy minerals	1	–
Clay	95	95
Radiolarians	0.5	–
Sponge spicules	0.5	5

GRAIN SIZE

	1-103
Sand	0.7
Silt	49.3
Clay	50.0

ORGANIC CARBON AND CARBONATE

	1-50
% Organic Carbon	0.2
% $CaCO_3$	0

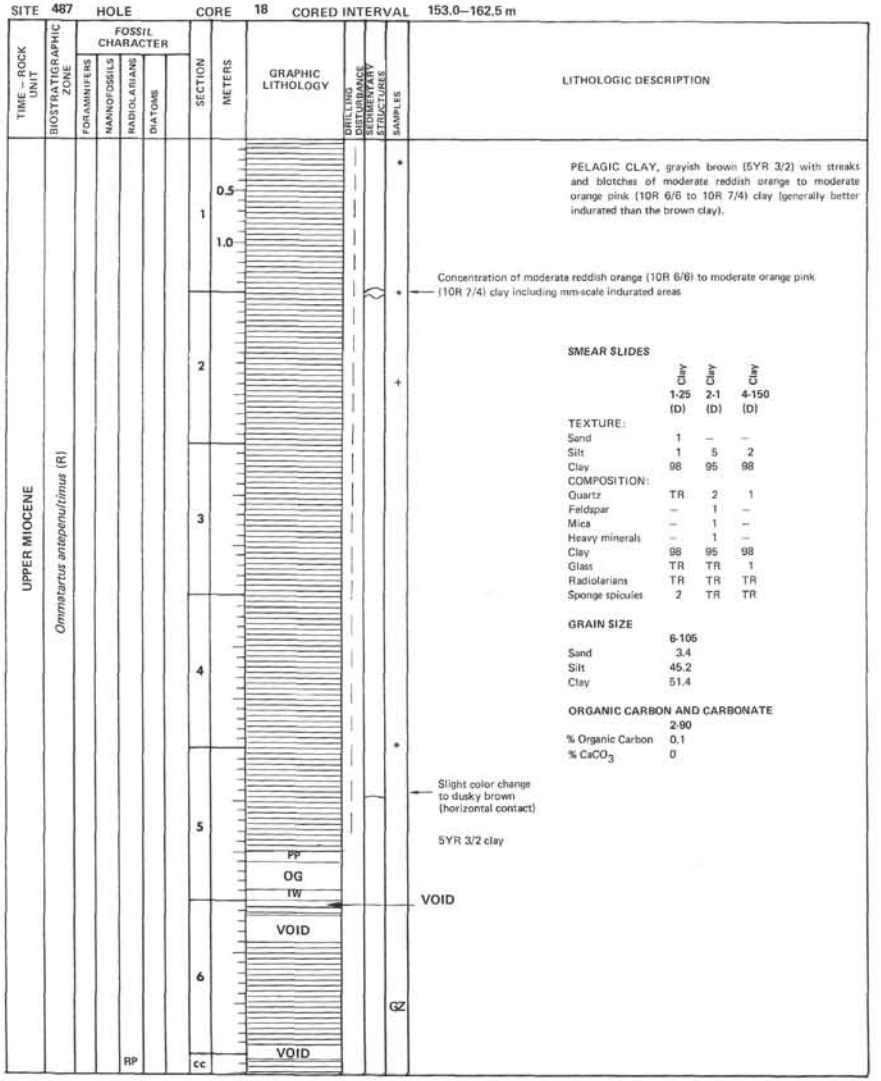
SITE 487 HOLE CORE 18 CORED INTERVAL 153.0–162.5 m
TIME – ROCK UNIT
BIOSTRATIGRAPHIC ZONE
FOSSIL CHARACTER
FORAMINIFERS
NANNOFOSSILS
RADIOLARIANS
DIATOMS
SECTION
METERS
GRAPHIC LITHOLOGY
DRILLING DISTURBANCE
SEDIMENTARY STRUCTURES
SAMPLES
LITHOLOGIC DESCRIPTION
UPPER MIOCENE
Ommatartus antepenultimus (R)
RP
PELAGIC CLAY, grayish brown (5YR 3/2) with streaks and blotches of moderate reddish orange to moderate orange pink (10R 6/6 to 10R 7/4) clay (generally better indurated than the brown clay).
Concentration of moderate reddish orange (10R 6/6) to moderate orange pink (10R 7/4) clay including mm-scale indurated areas
SMEAR SLIDES
Clay 1-25 (D)
Clay 2-1 (D)
Clay 4-150 (D)
TEXTURE:
Sand 1 – –
Silt 1 5 2
Clay 98 95 98
COMPOSITION:
Quartz TR 2 1
Feldspar – 1 –
Mica – 1 –
Heavy minerals – 1 –
Clay 98 95 98
Glass TR TR 1
Radiolarians TR TR TR
Sponge spicules 2 TR TR
GRAIN SIZE
6-105
Sand 3.4
Silt 45.2
Clay 51.4
ORGANIC CARBON AND CARBONATE
2-90
% Organic Carbon 0.1
% CaCO3 0
Slight color change to dusky brown (horizontal contact)
5YR 3/2 clay
PP
OG
IW
VOID
VOID
VOID
GZ
cc

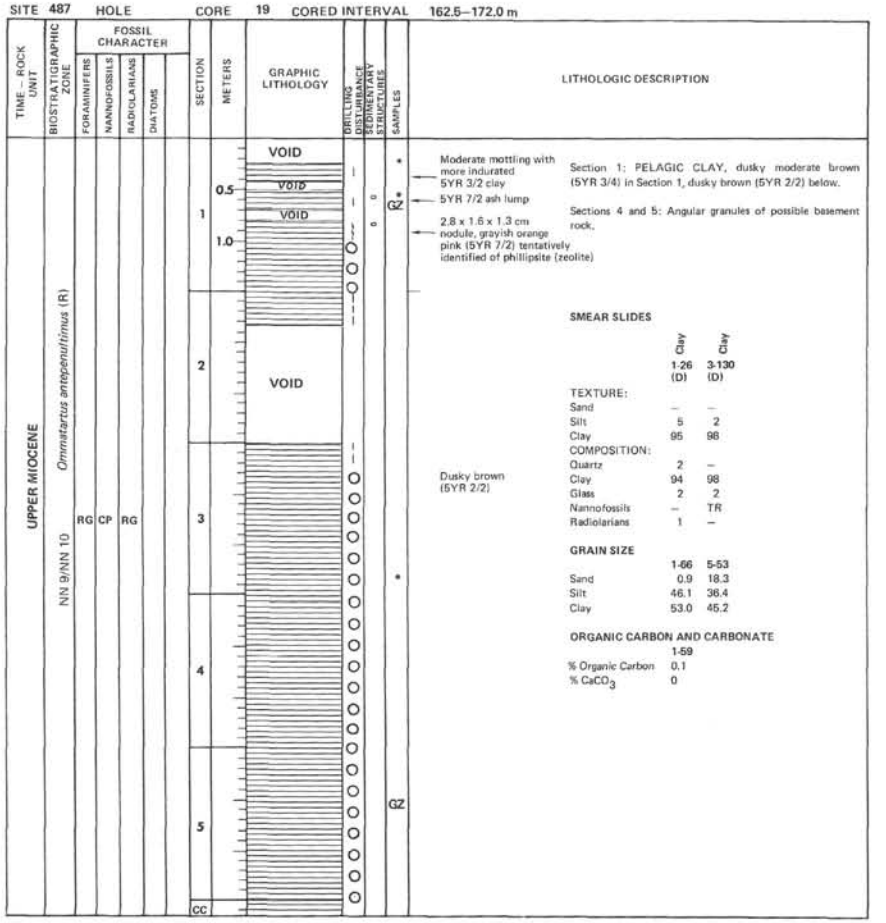
SITE 487 HOLE CORE 19 CORED INTERVAL 162.5–172.0 m
TIME – ROCK UNIT
BIOSTRATIGRAPHIC ZONE
FOSSIL CHARACTER
FORAMINIFERS
NANNOFOSSILS
RADIOLARIANS
DIATOMS
SECTION
METERS
GRAPHIC LITHOLOGY
DRILLING DISTURBANCE
SEDIMENTARY STRUCTURES
SAMPLES
LITHOLOGIC DESCRIPTION
UPPER MIOCENE
Ommatartus antepenultimus (R)
NN 9/NN 10
RG CP RG
VOID
VOID
VOID
VOID
GZ
cc
Moderate mottling with more indurated 5YR 3/2 clay
5YR 7/2 ash lump
2.8 x 1.6 x 1.3 cm nodule, grayish orange pink (5YR 7/2) tentatively identified of phillipsite (zeolite)
Dusky brown (5YR 2/2)
Section 1: PELAGIC CLAY, dusky moderate brown (5YR 3/4) in Section 1, dusky brown (5YR 2/2) below.
Sections 4 and 5: Angular granules of possible basement rock.
SMEAR SLIDES
Clay 1-26 (D)
Clay 3-130 (D)
TEXTURE:
Sand – –
Silt 5 2
Clay 95 98
COMPOSITION:
Quartz 2 –
Clay 94 98
Glass 2 2
Nannofossils – TR
Radiolarians 1 –
GRAIN SIZE
1-66
5-53
Sand 0.9 18.3
Silt 46.1 36.4
Clay 53.0 45.2
ORGANIC CARBON AND CARBONATE
1-59
% Organic Carbon 0.1
% CaCO3 0

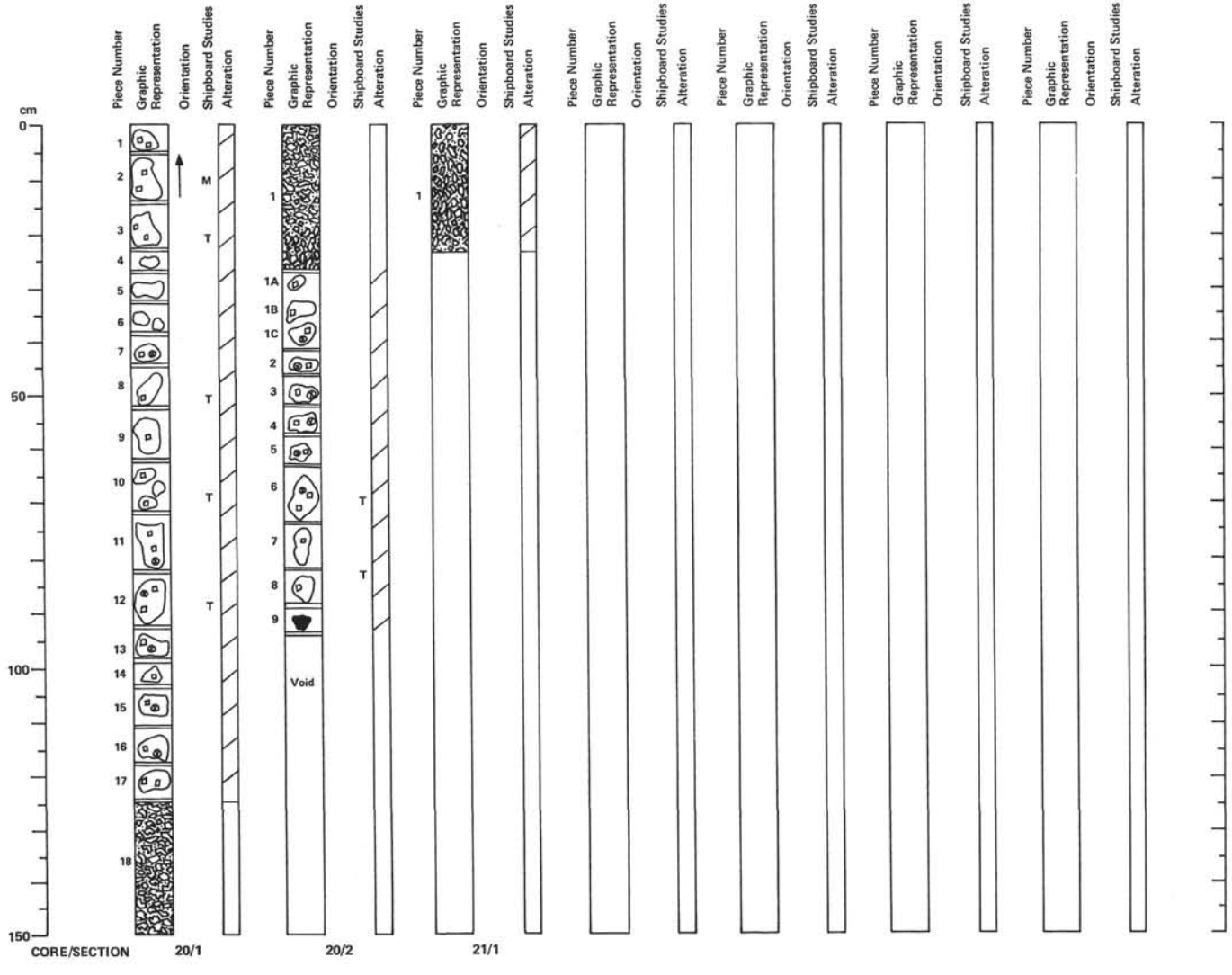

SITE 487, CORE 20, SECTION 1, 172.0–173.5 m

Macroscopic Description

Fine-grained plagioclase-olivine phyric to aphyric basalt. Small variolites present in Pieces 7, 11, 12, 13, 15, and 16; glass present only in one piece of Section 2. Pieces 4, 5, and 6 are aphyric. Plagioclase phenocrysts form up to 5% of the basalt, and are up to 4 mm across. Olivine phenocrysts are rare (0–1%), up to 2 mm across, and are often altered to light orange secondary minerals. The basalt is slightly to moderately altered throughout, with brown alteration zones rimming fractures. No interbedded sediments were recovered; granular material at 122–150 cm is probably drilling rubble composed of sediment and small basalt fragments which are stratigraphically out of place and intermixed by drilling.

Thin Section Description

16–20 cm (Piece 3), 43–49 cm (Piece 8), 63–66 cm (Piece 10), and 81–86 cm (Piece 12): Sparsely phyric plagioclase-olivine basalt to aphyric basalt.

Texture: Sparsely porphyritic, with intersertal groundmass (Piece 8 is aphyric and intersertal).

Phenocrysts: Plagioclase TR–5% (1–4 mm); olivine 0–TR% (up to 1.5 mm); glomeroporphyritic clusters of plagioclase and olivine, often somewhat resorbed and rounded; plagioclase phenocrysts often contain inclusions of glass and rarely euhedral chrome spinel.

Groundmass: Olivine 3–10% (0.02–0.1 mm), euhedral to subhedral, occasionally at centers of clusters of radiating plagioclase laths; plagioclase 25–40% (0.05–0.3 mm), euhedral to subhedral laths, acicular needles, rarely skeletal; clinopyroxene 20–35% (up to 0.3 mm), generally very fine-grained, often as dendritic intergrowths with titanomagnetite dust and minute plagioclase needles, occasionally skeletal; titanomagnetite 2% (up to 0.05 mm), dust and small skeletal crystals; glass 14–36%, partially altered to palagonite and clays.

Vesicles: <1–1% (up to 0.2 mm), generally partially filled by clays.

Alteration: Palagonite (up to 5%) and clays (< 1%) replacing glass, and iddingsite (< 1%) and minor clays partially replacing olivine.

SITE 487, CORE 20, SECTION 2, 173.5–181.5 m

Macroscopic Description

General description given in Section 1. Small variolites present in Pieces 1C, 2, 3, 4, 5, and 6 (25–75 cm); Piece 9 (88–91 cm) is the only glass recovered in Core 20.

Thin Section Description

68–70 cm (Piece 6) and 81–84 cm (Piece 8): Sparsely phyric plagioclase-olivine basalt.

Texture: Porphyritic with an intersertal groundmass.

Phenocrysts: Plagioclase 2–3% (1–4 mm); olivine < 1% (up to 1 mm); glomeroporphyritic clusters of plagioclase ± olivine, clusters somewhat rounded, plagioclase phenocrysts contain abundant glass inclusions and rare euhedral chrome spinel inclusions.

Groundmass: olivine 8% (up to 0.1 mm), euhedral; plagioclase 30–35% (up to 0.3 mm), euhedral to subhedral laths, acicular needles, rarely skeletal; clinopyroxene 30–35% (up to 0.2 mm), generally very fine grained, often dendritic intergrowths with titanomagnetite dust and minute plagioclase needles, occasionally skeletal; titanomagnetite 5–7% (up to 0.05 mm), fine-grained dust; glass 15–17%, partially palagonitized.

Vesicles: 2%, void to partially filled by clays.

Alteration: Trace of palagonite replacing glass.

SITE 487, CORE 21, SECTION 1, 181.5–191.0 m

Macroscopic Description

Drilling rubble, mostly basalt fragments, and clasts (rare) of zeolite (phillipsite).

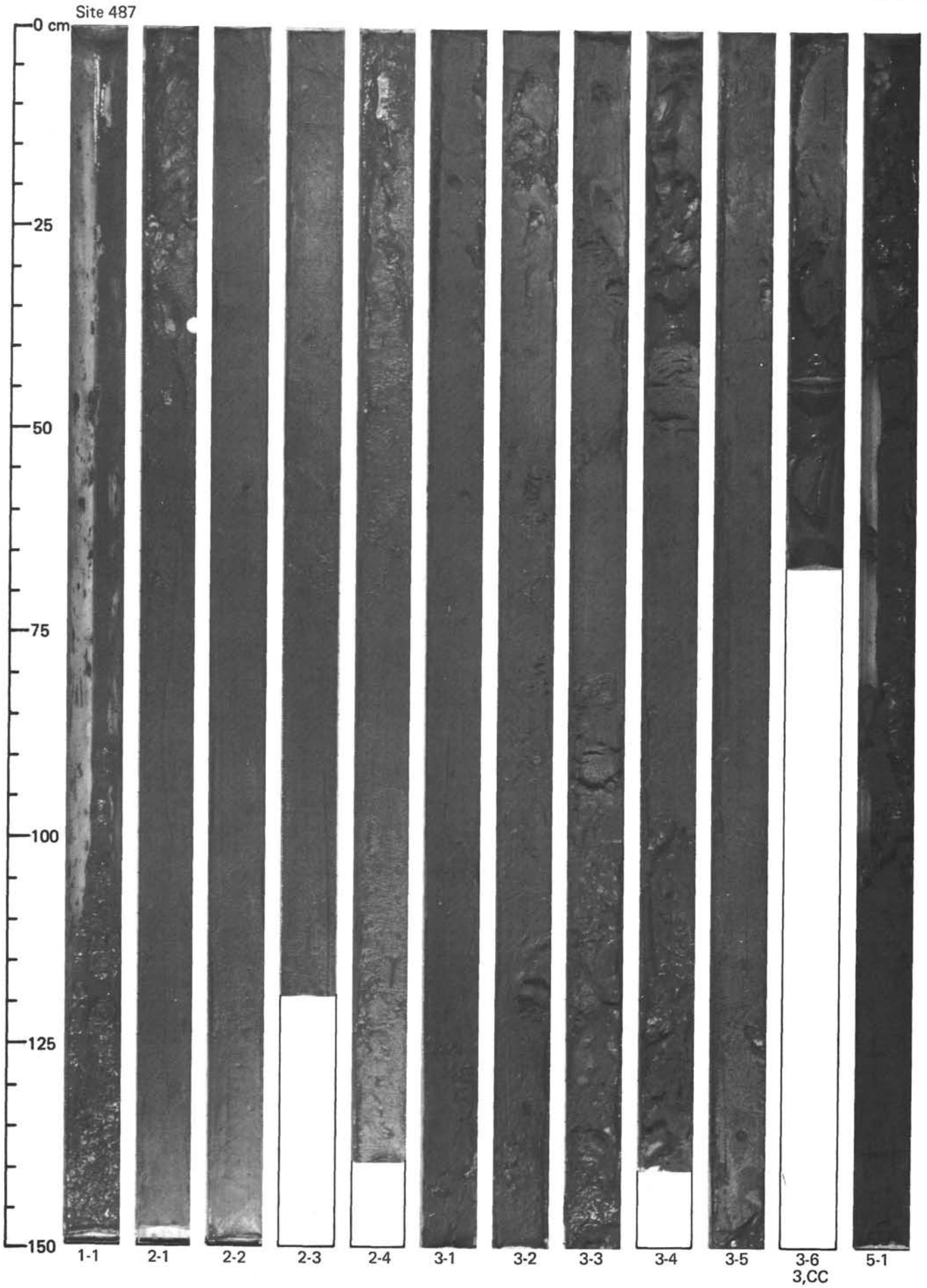
Site 487
0 cm
25
50
75
100
125
150
1-1
2-1
2-2
2-3
2-4
3-1
3-2
3-3
3-4
3-5
3-6
3,CC
5-1

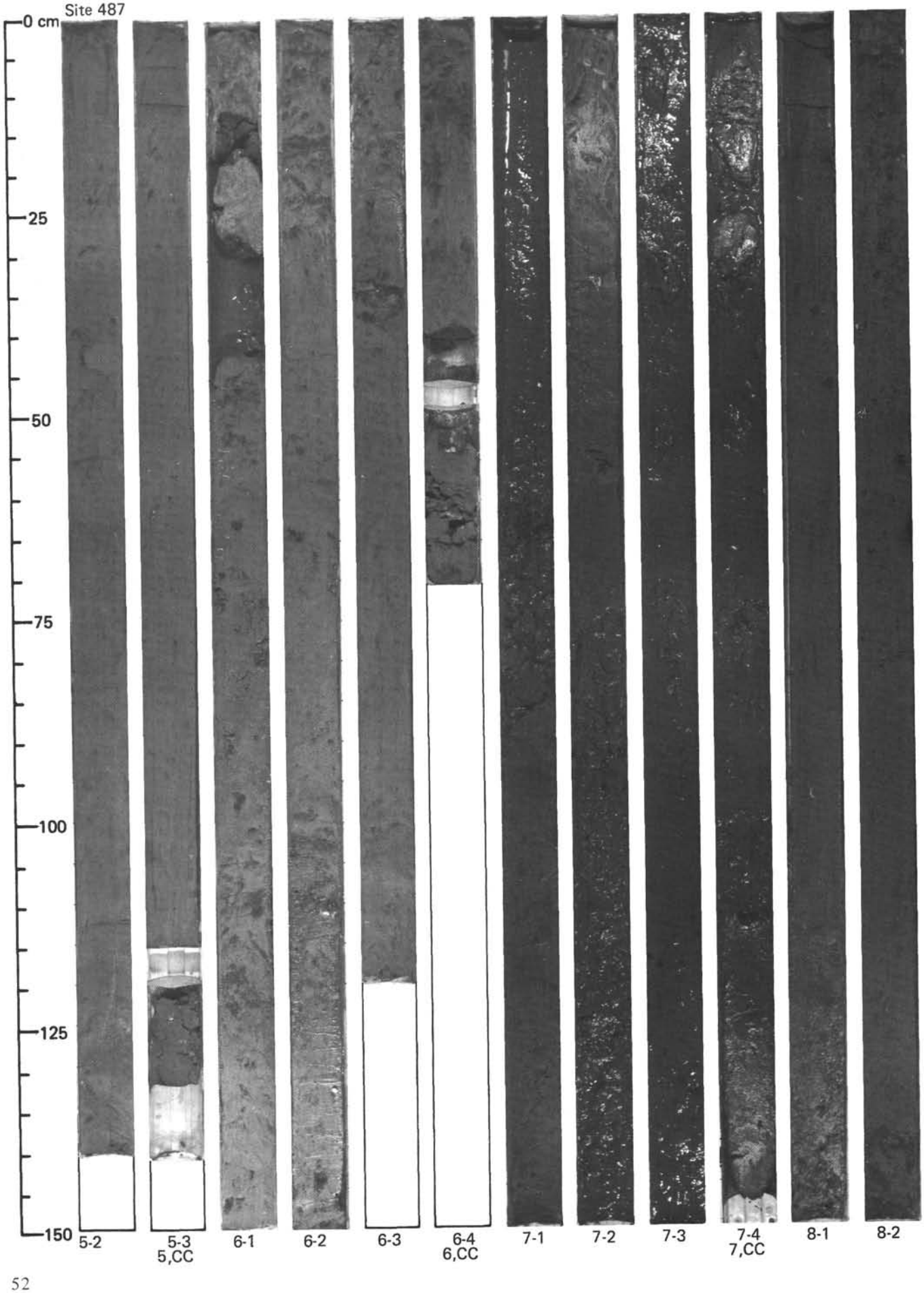
Site 487
0 cm
25
50
75
100
125
150
5-2
5-3
5,CC
6-1
6-2
6-3
6-4
6,CC
7-1
7-2
7-3
7-4
7,CC
8-1
8-2

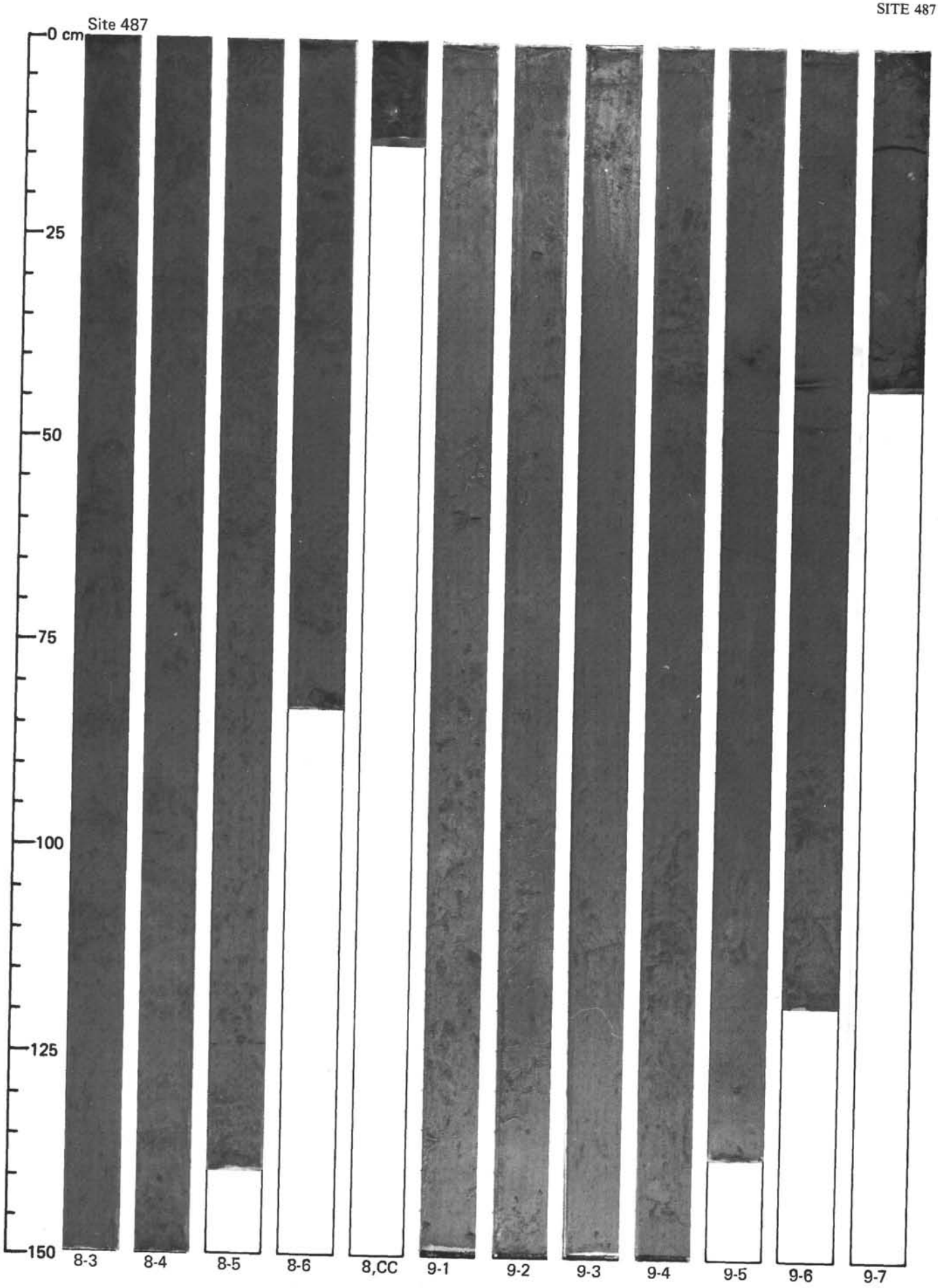
Site 487
0 cm
25
50
75
100
125
150
8-3
8-4
8-5
8-6
8,CC
9-1
9-2
9-3
9-4
9-5
9-6
9-7

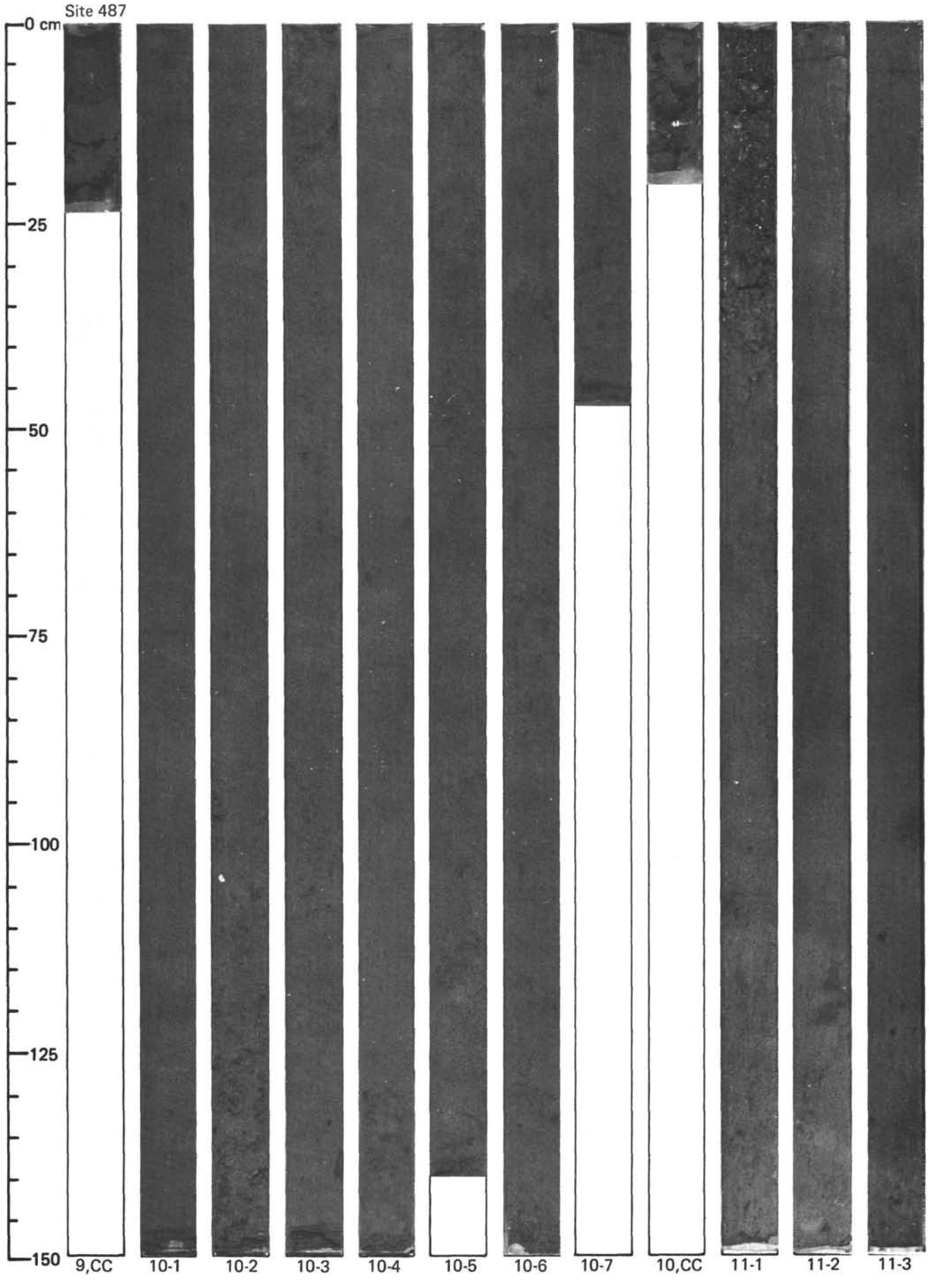
Site 487
0 cm
25
50
75
100
125
150
9,CC
10-1
10-2
10-3
10-4
10-5
10-6
10-7
10,CC
11-1
11-2
11-3

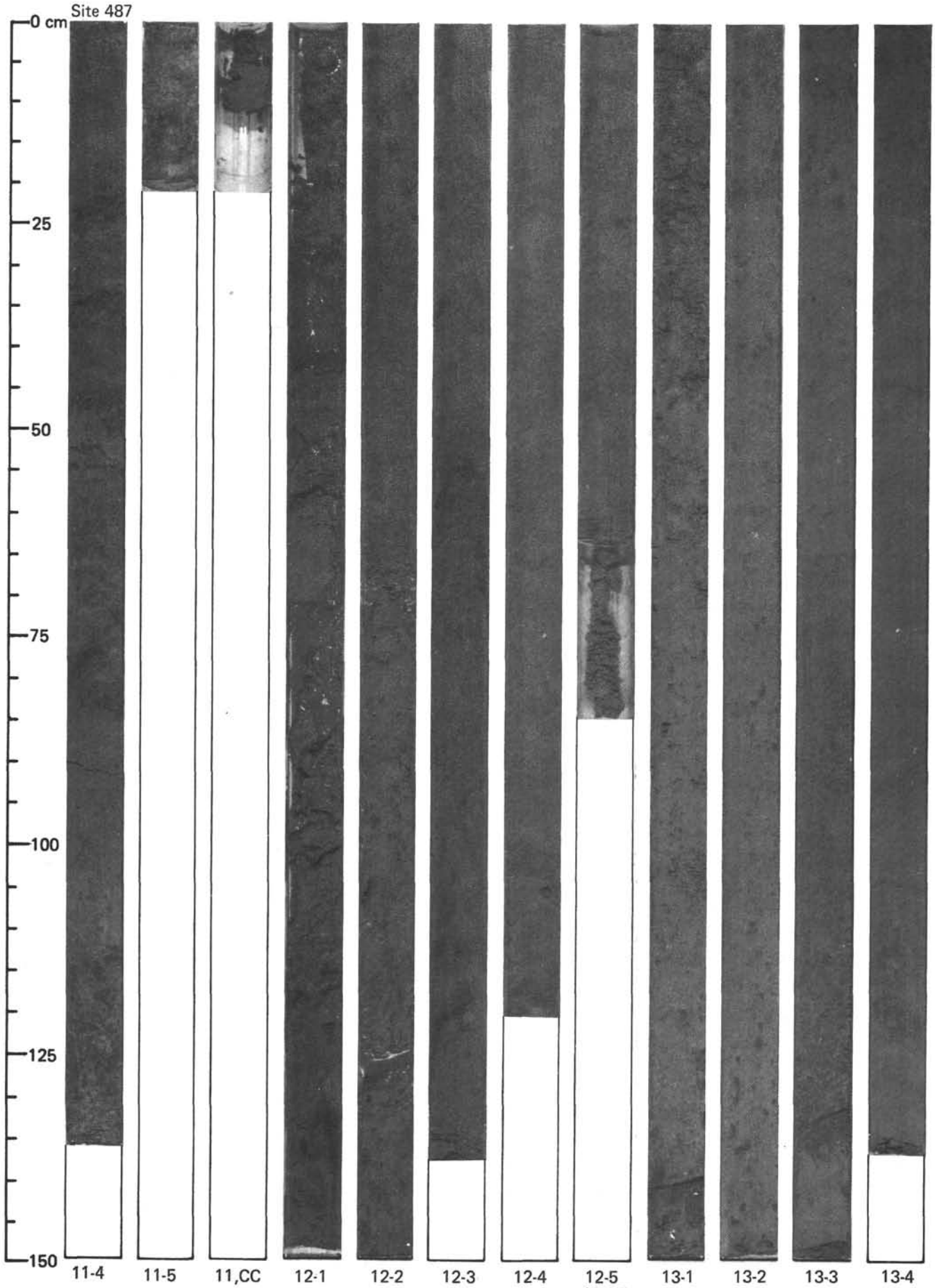
Site 487
0 cm
25
50
75
100
125
150
11-4
11-5
11,CC
12-1
12-2
12-3
12-4
12-5
12,CC
13-1
13-2
13-3
13-4

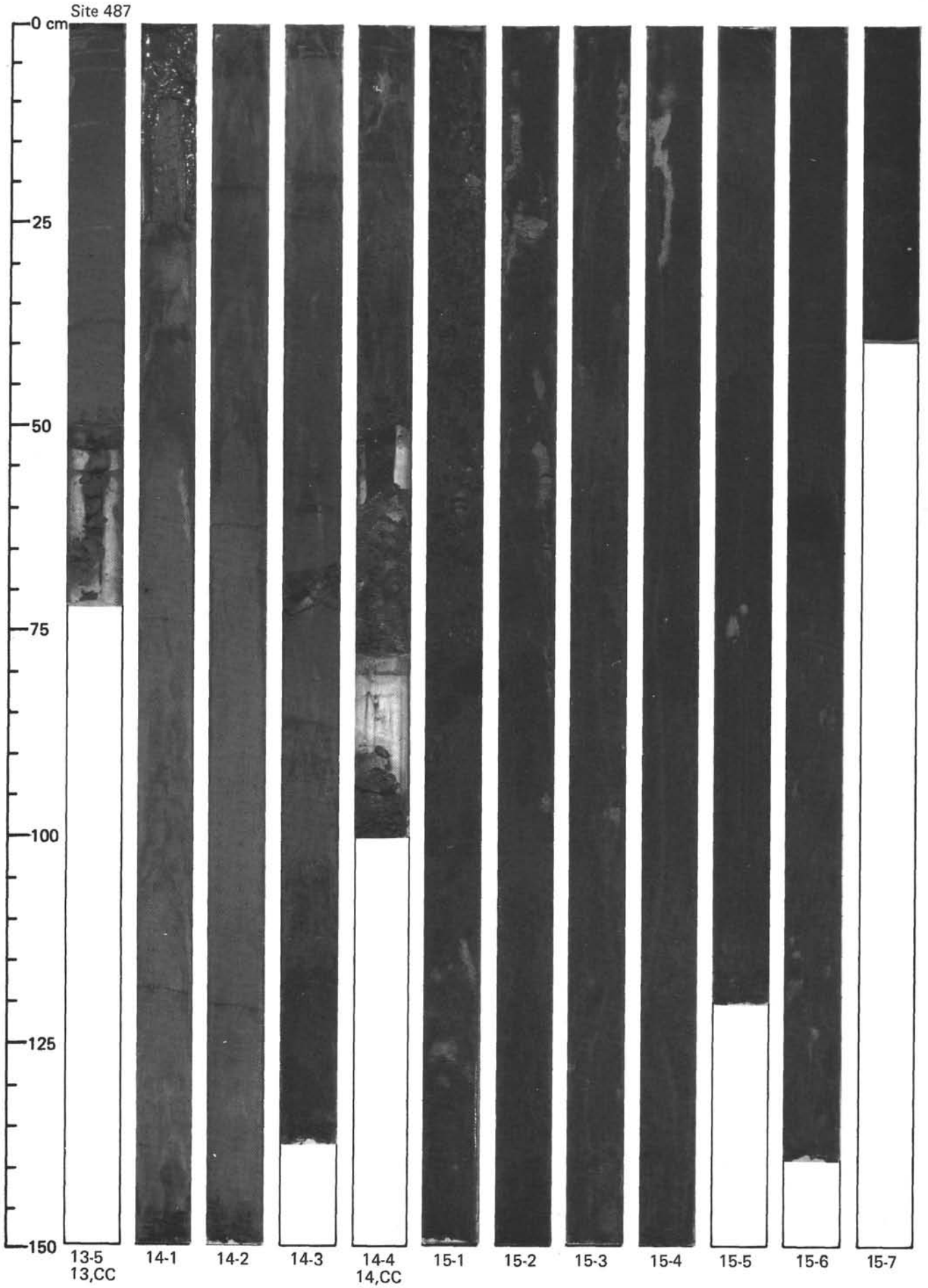
Site 487
0 cm
25
50
75
100
125
150
13-5
13,CC
14-1
14-2
14-3
14-4
14,CC
15-1
15-2
15-3
15-4
15-5
15-6
15-7

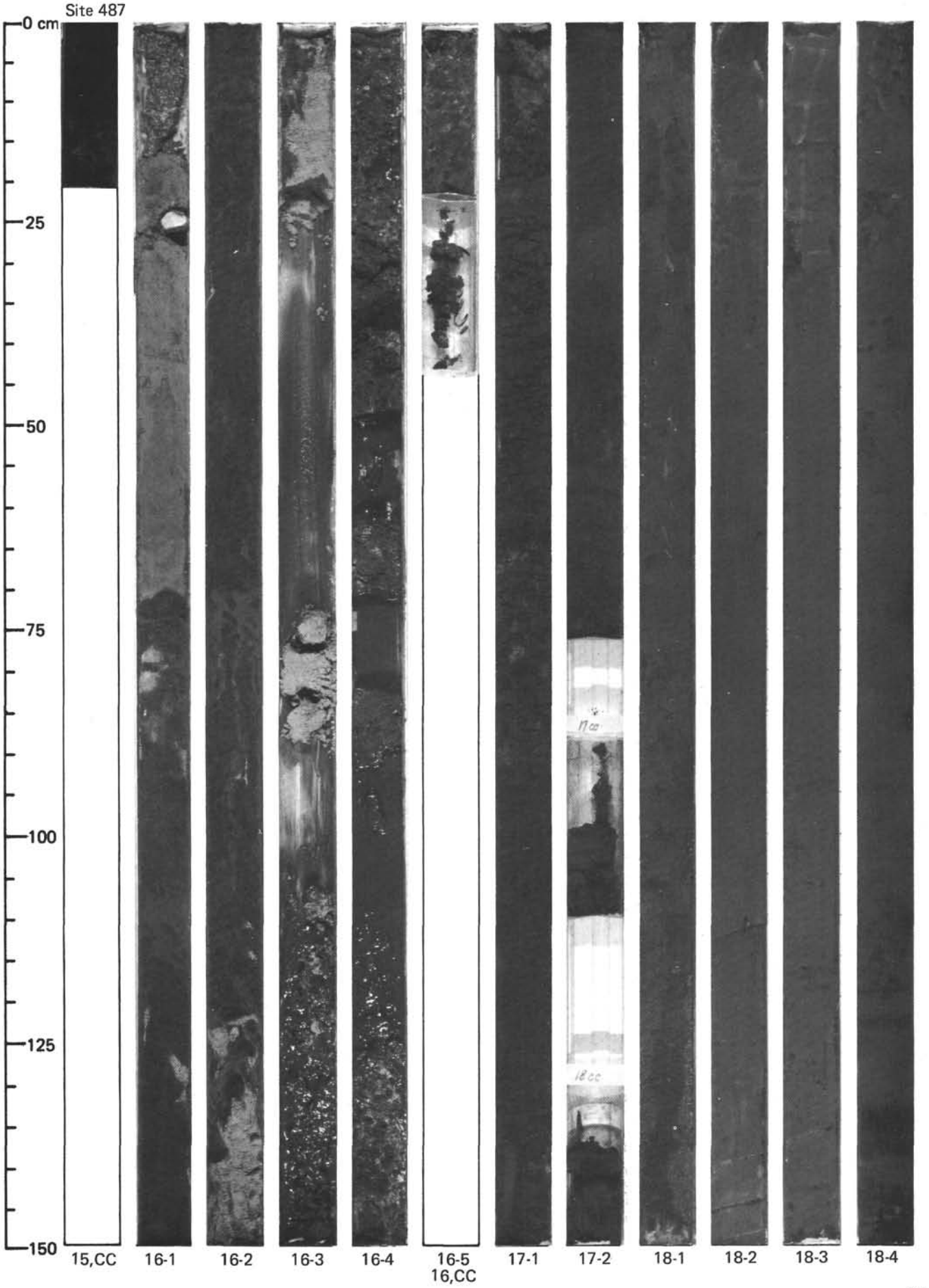
Site 487
0 cm
25
50
75
100
125
150
15,CC
16-1
16-2
16-3
16-4
16-5
16,CC
17-1
17-2
18-1
18-2
18-3
18-4

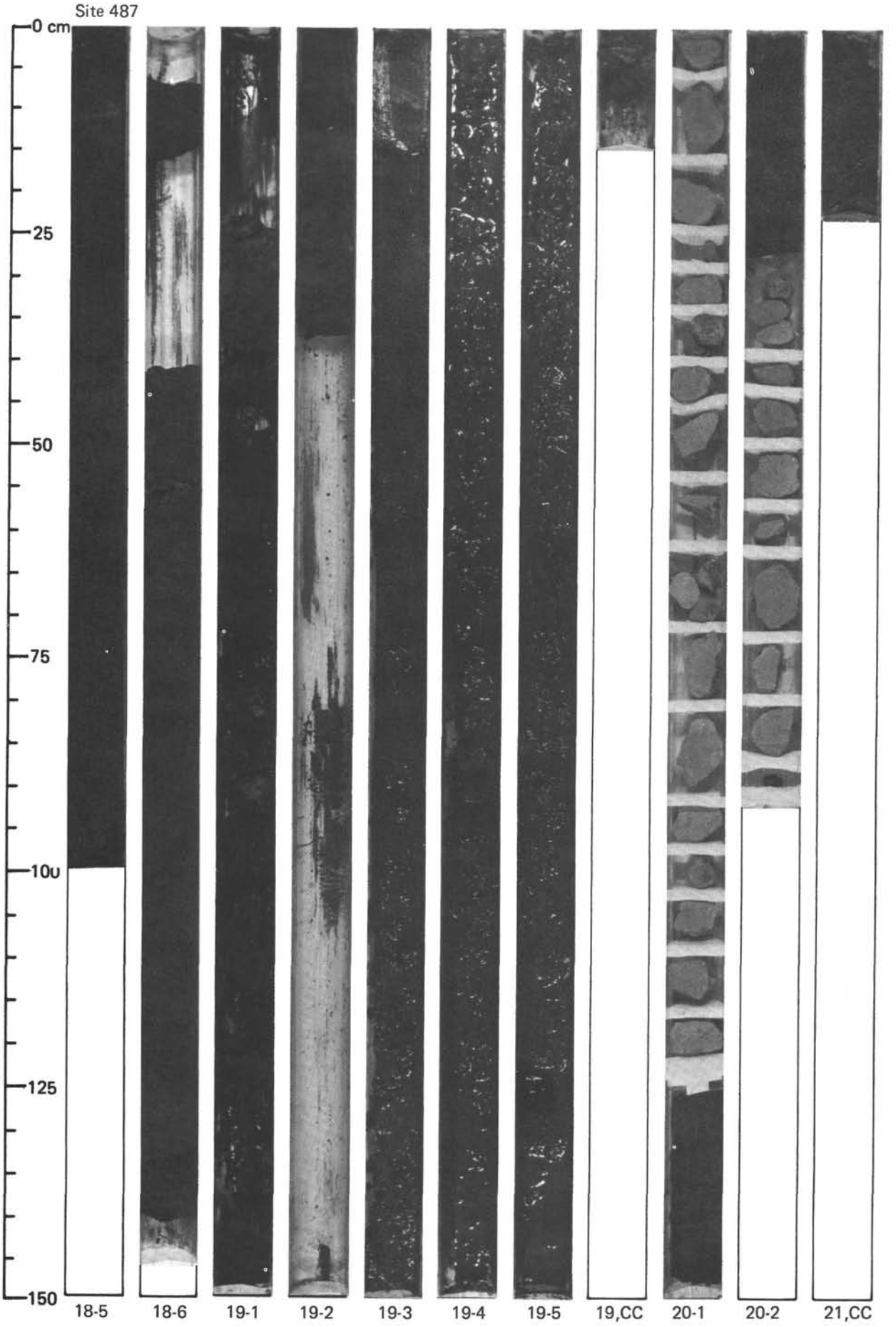
Site 487
0 cm
25
50
75
100
125
150
18-5
18-6
19-1
19-2
19-3
19-4
19-5
19,CC
20-1
20-2
21,CC